SOCIETY OF PETROLEUM ENGINEERS OF AIME
6200 North Central Expressway
Dallas, Texas 75206

PAPER NUMBER SPE 1721

THIS IS A PREPRINT --- SUBJECT TO CORRECTION

A Strength Criterion for Anisotropic Rocks Based Upon Experimental Observations

By

R. T. McLamore*, Jr. Member AIME, Texas Petroleum Research Committee, Austin, Tex., and K. E. Gray, Member AIME, U. of Texas, Austin, Tex.

ABSTRACT

Compressive strengths as a function of confining pressure and sample orientation were determined for three anisotropic rocks that possessed two distinctive types of anisotropic features: (1) cleavage planes (slate); (2) bedding planes (two types of Green River shale). The samples were tested over a confining pressure range of 1000 to 40,000 psi, with pore pressure held constant at atmospheric pressure. The orientation of the plane of anisotropy (bedding or cleavage plane) was varied between 0° and 90° relative to the axial stress. The compressive strength of all three rocks was found to be highly anisotropic. Maximum values of strength occurred at orientations of 0° and 90°, while minimum value occurred at an orientation of 30° for the Green River shale. The orientation of the minimum compressive strength for slate was found to be dependent upon the initial stress state.

The test results indicate that anisotropic rocks fail or deform by one of three mechanisms: (1) shear faulting (across or parallel to the bedding or cleavage plane); (2) plastic slip along the bedding or cleavage plane; (3) internal buckling (kinking). It was found that the failure mechanism was a function of both the initial stress state and the orientation of the plane of anisotropy relative to the axial stress.

Three current failure theories for anisotropic rocks--(1) the Walsh-Brace modification of Griffith's tensile failure theory; (2) Jaeger's single plane of weakness theory based on the Mohr-Coulomb theory; (3) Jaeger's continuously variable shear strength theory, also based on the Mohr-Coulomb theory--were analyzed and compared to the experimental strength data. It was found that the Walsh-Brace and the single plane of weakness theories predict identical failure criteria and could only be used successfully to describe the compressive strength behavior of the Green River shale. Jaeger's continuously variable shear strength theory could only be used to describe the compressive strength characteristics of the slate over a limited range of orientations.

The experimental data indicated that both the cohesive strength, τ_o, and the coefficient of internal friction, $\tan \phi$, may vary with respect to orientation for a given anisotropic rock. It was noted that the nature of the

*Now associated with Shell Dev. Co.

References and illustrations at end of paper.

variance of τ_o and tan ϕ was a function of the type of anisotropy (bedding or cleavage) present within the rock. An empirical relationship, based on the experimental data observed, that describes the variance of τ_o and tan ϕ as a function of the type of anisotropy has been proposed to use in conjunction with the Mohr-Coulomb theory as a compressive strength criterion for anisotropic rocks. It was found that this empirical criterion produced a good fit of the experimental data for all orientations and could be used to describe the strength behavior of both types of anisotropic rock studied.

Tensile strengths as a function of orientation were determined, using the indirect or "Brazilian" test technique, for one type of the Green River shale used in the compressive strength study. It was found that the tensile strength of the material was highly dependent upon the orientation of the bedding plane relative to the induced tensile stress and that the nature of this variation could be predicted by the modified Griffith failure criterion. It was also determined that the tensile strength of Green River shale is insensitive to confining pressure.

INTRODUCTION

Engineers and geophysicists are constantly being confronted with the need to know the strength of geological material at specific conditions of stresses and temperature as well as to predict the relative changes in strength as these two parameters vary. In the past, the great preponderance of literature dealing with the strength of and strength criteria for rocks has dealt with isotropic materials. Since the majority of the materials we work with on a day-to-day basis in oil well drilling, mining, seismic evaluation, and hydraulic fracturing are anisotropic in nature, the need for an adequate strength criterion for anisotropic rock is paramount. The small amount of experimental work performed on anisotropic rock in the past has in itself been insufficient to answer the many question pertaining to the role that the initial type of petrographical anisotropy plays in the mechanical behavior of the material.

In this paper we will report the effects of two types of petrographical anisotropy, cleavage and bedding, on the mechanical behavior of the material and present a new approach to predict the strength behavior of anisotropic rock. The strength criterion reported herein relates the compressive strength to the magnitude of the initial stress state, the orientation of the material relative to the minimum principal stress, and the petrographical nature of the rock itself.

STRENGTH CRITERIA FOR ANISOTROPIC ROCK

As of today, only four fracture criteria have been proposed for anisotropic rocks. In 1960, Jaeger[1] proposed two fracture criteria for anisotropic rocks based on generalizations of the Mohr-Coulomb theory for isotropic rocks. The first theory, known as the "single plane of weakness" theory, considers an isotropic body that possesses a plane or parallel planes of weakness. The second theory proposed by Jaeger is called the "continuously variable shear strength" theory and assumes that the rock parameter τ_o, cohesive strength, is a function of the orientation of the anisotropic nature of the rock relative to the applied stress.

The third fracture criterion was proposed by Walsh and Brace[2] and is an extension of the McClintock and Walsh[3] modification of Griffith's[4] tensile failure theory. It describes a material that possesses nonrandomly oriented Griffith cracks that close under loading.

The fourth fracture criterion, derived independently by Hoek,[5] is also a modification of Griffith theory and is essentially identical to the Walsh-Brace theory.

A brief summary of the first three theories listed follows. It will also be shown that the Walsh-Brace theory and Jaeger's single plane of weakness theory are identical in final form even though the fracture mechanisms involved are quite different in nature.

Walsh-Brace Theory

The Walsh-Brace theory[2] assumes that failure is tensile in nature and that the body is composed of long, nonrandomly oriented cracks that are superposed on an isotropic array of randomly distributed smaller cracks. The long as well as the short crack arrays are such that the cracks close at relatively low values of applied stress thus transmitting both normal and shearing stresses. Fracture is assumed to occur when the local tensile stress at the tip of the crack exceeds the inherent tensile strength of the material. Walsh and Brace assume that fracture may occur through the growth of either the long or the small cracks depending upon the orientation of the long crack system to the applied load $(\sigma_3 - \sigma_1)$. The fracture stress, $(\sigma_3 - \sigma_1)$, required for fractures originating at the small, randomly oriented cracks is given for any confining pressure, σ_1, by

$$(\sigma_1 - \sigma_3)_s = C_{o\,s} + \frac{2\mu_s \sigma_1}{(1 + \mu_s^2)^{\frac{1}{2}} - \mu_s} \quad . \quad . \quad [1]$$

where C_{o_s} is the atmospheric compressive strength of the randomly oriented short crack material and μ_s is the coefficient of friction for the short cracks. If fracture occurs as a result of the growth of the long crack system, which is oriented at an angle β to σ_3, then the fracture stress, $(\sigma_1 - \sigma_3)$, at any confining pressure, σ_1, is given by

$$(\sigma_1 - \sigma_3)_L = \frac{C_{o_L}[(1 + \mu_L^2)^{\frac{1}{2}} - \mu_L] + 2\mu_L\sigma_1}{2 \sin \beta \cos \beta(1 - \mu_L \tan \beta)} , \quad [2]$$

where C_{o_L} is the atmospheric compressive strength for the most critical orientation of β, say 30°, and μ_L is the coefficient of friction for the long cracks.

Four parameters, C_{o_L}, C_{o_s}, μ_L, and μ_s, must be determined in order to evaluate this theory. The value of C_{o_s} is found by determining the atmospheric compressive strength for samples with orientations of 0° and 90°. The value of C_{o_L} is found by determining the minimum value of the atmospheric compressive strength as the orientation of the sample is varied. This orientation usually occurs around 30°.

The friction coefficients μ_s and μ_L can be determined by running a series of compression tests at various confining pressures and fixed orientations, say 0° and 90° for μ_s and 30° for μ_L. The slope of the compressive strength versus confining pressure plot for any orientation is equal to $2\mu_{L,s}/[(1+\mu_{L,s}^2)^{\frac{1}{2}} - \mu_{L,s}]$, where the subscripts refer to the particular orientation and crack system.

The values of μ_s and C_{o_s} should be determined for both the 0° and 90° orientation and the corresponding fracture strength calculated for both cases as a function of confining pressure, since it has been noted that the fracture strengths at these two orientations, which represent failure due to the short crack system, are not necessarily identical.

Once the parameters μ_s, μ_L, C_{o_s}, and C_{o_L} have been determined, the theory may be evaluated by calculating the values of $(\sigma_1 - \sigma_3)_s$ and $(\sigma_1 - \sigma_3)_L$, using equations [1] and [2], for a given confining pressure and orientation and using the smaller of the two values as the fracture strength.

Single Plane of Weakness Theory

As opposed to the Walsh-Brace theory which assumes failure occurs due to local tensile stress, the single plane of weakness theory, proposed by Jaeger,[1] assumes that the body fails in shear. This theory is a generalization of the well-known Mohr-Coulomb linear envelope failure theory and describes an isotropic body that contains a single plane or a system of parallel planes of weakness. The failure of the matrix material is given by

$$\tau = \tau_o - \sigma \tan \phi , \quad [3]$$

where τ_o is the cohesive strength of the matrix material and $\tan \phi$ is the coefficient of friction. Failure along the plane of weakness is described by

$$\tau = \tau_o' - \sigma \tan \phi' \quad [4]$$

Using the well-known Mohr circle relationship that relates τ and σ to σ_1, σ_3, and the angle of internal friction, ϕ, the final form of the single plane of weakness theory can be derived from equations [3] and [4].

For failure within the matrix, the equation is

$$(\sigma_3 - \sigma_1) = \frac{2\tau_o - 2\sigma_1 \tan \phi}{[\tan \phi - \sqrt{1 + \tan^2 \phi}]} \quad [5]$$

or

$$(\sigma_3 - \sigma_1) = C_o + \frac{2\sigma_1 \tan \phi}{\sqrt{\tan^2 \phi + 1} - \tan \phi} , \quad [6]$$

where C_o is the atmospheric compressive strength of the material.

The fracture strength of the material in the plane of weakness is given by

$$(\sigma_3 - \sigma_1) = \frac{2\tau_o - 2\sigma_1 \tan \phi'}{\tan \phi'(1 - \cos 2\beta) - \sin 2\beta} , \quad [7]$$

where β is the angle between σ_3 and the plane of anisotropy and in both cases σ_1 represents the confining pressure.

The theory is evaluated by running tests at 0°, 90°, and 30° orientation for various confining pressures, plotting linear Mohr-Coulomb envelopes and determining the value of the parameters ϕ, ϕ', τ_o, and τ_o'. Once these parameters have been evaluated, the fracture strength is calculated for a certain pressure and orientation using equations [5] and [7] with the lowest value taken as the strength of the material. The same argument made in the previous section relative to the matrix strength near the 0° and 90° orientation is true here also, and fracture strengths should be calculated for both of these orientations to determine the strength of the matrix on either side of the area of anisotropic strength behavior.

Comparison of the Single Plane of Weakness Theory and the Walsh-Brace Theory

Inspection of equations [5] and [6] shows that the relationship between the fracture stress, $(\sigma_3 - \sigma_1)$, and the confining pressure, σ_1, for a fixed value of β is a straight line that has a slope m equal to

$$m = \frac{2 \tan \phi}{\sqrt{\tan^2 \phi + 1} - \tan \phi} \quad \ldots\ldots [8]$$

and an intercept on the $(\sigma_3 - \sigma_1)$ axis of

$$C_o = \frac{2\tau_o}{\tan \phi - \sqrt{1 + \tan^2 \phi}} , \quad \ldots [9]$$

where C_o is the atmospheric compressive strength.

By solving equation [8] for tan ϕ, it can be seen that

$$\tan \phi \big|_{\beta=\text{fixed}} = \left[\frac{m^2}{4(m+1)}\right]^{\frac{1}{2}} \quad \ldots [10]$$

Recall that for a fixed value of β the slope of the confining pressure - fracture strength curve is given by

$$m = \frac{2\mu}{[(1 + \mu^2)^{\frac{1}{2}} - \mu]} \quad \ldots\ldots [11]$$

Thus

$$\mu \big|_{\beta=\text{fixed}} = \left[\frac{m^2}{4(m+1)}\right]^{\frac{1}{2}} \quad \ldots\ldots [12]$$

From even a cursory comparison of equations [12] and [10], it is obvious that the two frictional parameters tan ϕ and μ are equivalent. In view of the fact that μ_s and tan ϕ are evaluated from compression tests run at an orientation of 0° or 90° and μ_L and tan ϕ' are evaluated from tests run at β = 30°, it is apparent that

$$\mu_s = \tan \phi , \quad \ldots\ldots [13]$$

$$\mu_L = \tan \phi' , \quad \ldots\ldots [14]$$

and, in general, for any given orientation of β

$$\mu = \tan \phi \quad \ldots\ldots [15]$$

Recall equation [1]

$$(\sigma_3 - \sigma_1) = C_{o_s} + \frac{2\mu_s \sigma_1}{\sqrt{1 + \mu_s^2} - \mu_s} , \quad \ldots [1]$$

which is the fracture criterion predicted by the Walsh-Brace theory for the orientations of β where failure occurs due to growth of the short crack system. C_{o_s} is the atmospheric compressive stress for β = 0° or 90°.

Recall also equation [6]

$$(\sigma_3 - \sigma_1) = C_o + \frac{2\sigma_1 \tan \phi}{\sqrt{1 + \tan^2 \phi} - \tan \phi} , \quad [6]$$

which is the fracture criterion predicted by the single plane of weakness theory for the orientations of β where failure occurs along planes predicted by the Mohr-Coulomb failure theory.

By comparing equations [1], [6], and [15], it is apparent that if C_o, C_{o_s}, tan ϕ, and μ_s are all determined from data run at the same orientation, either 0° or 90°, then the fracture criterions predicted by the two theories are identical for the range of β where the strength of material is not affected by the anisotropic nature of the material.

Equation [16] shows the relationship between τ_o and tan ϕ as determined from equation [9]

$$\tau_o = \frac{C_o}{2} (\tan \phi - \sqrt{\tan^2 \phi + 1}) \quad \ldots [16]$$

By substituting equations [15] and [16] into equation [7] and using the appropriate trigonometric identities, it can be shown, with some rearrangement, that the single plane of weakness theory and the Walsh-Brace theory are indeed identical over the entire range of β. The following development illustrates this fact.

Equation [17] is derived by combining equations [7], [15], and [16]

$$(\sigma_3 - \sigma_1) = \frac{C_o[\mu - (1 + \mu^2)^{\frac{1}{2}}] - 2\mu\sigma_1}{(1 - \cos 2\beta)\mu - \sin 2\beta} \quad [17]$$

Now, by substituting the following trigonometric relationships into equation [7]

$$\cos 2\beta = 1 - 2 \sin^2 \beta ,$$

$$\sin 2\beta = 2 \sin \beta \cos \beta ,$$

$$\frac{\sin \beta}{\cos \beta} = \tan \beta ,$$

the following development is generated:

$$(\sigma_3 - \sigma_1) = \frac{C_o[\mu - (1 + \mu^2)^{\frac{1}{2}}] - 2\mu\sigma_1}{2\mu \sin^2 \beta - 2 \sin \beta \cos \beta}$$

$$= \frac{C_o[\mu - (1 + \mu^2)^{\frac{1}{2}}] - 2\mu\sigma_1}{2 \sin\beta \cos\beta \frac{\sin\beta}{\cos\beta}\mu - 2 \sin\beta \cos\beta}$$

$$= \frac{C_o[\mu - (1 + \mu^2)^{\frac{1}{2}}] - 2\mu\sigma_1}{2 \sin\beta \cos\beta(\mu \tan\beta - 1)}$$

or

$$(\sigma_3 - \sigma_1) = \frac{C_o[(1 + \mu^2)^{\frac{1}{2}} - \mu] + 2\mu\sigma_1}{2 \sin\beta \cos\beta(1 - \mu \tan\beta)} \quad . \quad . \quad . \quad . \quad . \quad . \quad . \quad . \quad . \quad . \quad . \quad . \quad . \quad [18]$$

Equation [18] represents the fracture criterion, as predicted by the single plane of weakness theory, for the range of β where failure is controlled by the "plane of weakness." By comparing equations [18] and [2] and realizing that $\mu = \mu_L$ and $C_o = C_{oL}$, since they were determined from the same orientation, it is obvious that the two theories predict identical fracture criterions for the range of β where failure is controlled by the anisotropic nature of the material.

Thus the two theories, one based on shear failure and the other on the tensile failure associated with the growth of nonrandomly oriented Griffith cracks, are identical over the entire range of β. It should be noted here that prior to the publication of the McClintock-Walsh modification of Griffith's theory, Brace[6] showed that the equality between μ and tan ϕ did exist as related to the comparison of the McClintock-Walsh and Mohr-Coulomb theory. The analysis presented here is an extension of Brace's analysis and establishes the identity between the Walsh-Brace theory and the single plane of weakness theory proposed by Jaeger.

One of the more interesting relationships that can be derived, as a result of realizing that μ = tan ϕ, is an equation that relates the ratio of the atmospheric compressive strength-atmospheric tensile strength to the coefficient of internal friction for isotropic rocks.

McClintock and Walsh noted that the relationship between the fracture stress at $\sigma_1 = 0$ and μ, is given by

$$C_o = \frac{4K\sqrt{1 - \frac{\sigma_c}{K}} + 2\mu\sigma_c}{\mu - \sqrt{1 + \mu^2}} \quad , \quad . \quad . \quad . \quad . \quad [19]$$

where σ_c is the stress needed to close the Griffith cracks. They also observed that a value of $\sigma_c = 0$ generated theoretical curves that best fit the experimental data. By setting $\sigma_c = 0$ and substituting equation [15] into equation [19], the relationship between C_o/K and tan ϕ is found to be

$$\frac{C_o}{K} = \frac{4}{\tan\phi - \sqrt{1 + \tan^2\phi}} \quad . \quad . \quad . \quad . \quad [20]$$

The relationship between C_o/K and tan ϕ as predicted by the Mohr-Coulomb theory[22] is given by

$$\frac{C_o}{K} = \frac{\tan\phi + \sqrt{\tan^2\phi + 1}}{\tan\phi - \sqrt{\tan^2\phi + 1}} \quad . \quad . \quad . \quad . \quad [21]$$

The two relationships, equations [20] and [21], are presented in Figure 1 along with some experimental data obtained by Sykes,[8] Gnirk and Cheatham,[9] and Wuerker.[10] Very little experimental data have been published that correlate all three parameters, K, C_o, and tan ϕ, for a given isotropic rock and, as such, the data presented in Figure 1 do little to corroborate either the McClintock-Walsh or the Navier-Coulomb relationships. However, both relationships are realistic in that they predict the atmospheric compressive strength is either equal to or greater than the tensile strength of the rock at tan ϕ and that the ratio of the strengths increase as tan ϕ increases. Wuerker has reported average strength ratios that vary from around 3 to 85 for 11 rocks and values of tan ϕ from 0.5 ($\phi \cong 26.5°$) to 2.9 ($\phi \cong 71°$) for 46 various rocks. From these ranges of values, it is evident that both the Walsh-Brace and the single plane of weakness relationships for C_o/K are more realistic than the Griffith theory which predicts a constant value for C_o/K equal to 8.

The Continuously Variable Shear Strength Theory

The continuously variable shear strength theory was also proposed by Jaeger[1] and is based on the Mohr-Coulomb theory (linear Mohr envelope). The theory assumes that the cohesive strength of the material is a continuous function of β and can be described by

$$\tau_o = A - B \cos 2(\alpha - \beta) \quad , \quad . \quad . \quad . \quad [22]$$

where A and B are constants and α is the orientation of β for which τ_o is a minimum. (As in the case of the fracture strength, the minimum value of τ_o usually occurs at $\beta = \alpha = 30°$.)

The fracture criterion for the continuously variable shear strength theory can be derived by combining equations [5] and [22].

$$(\sigma_3 - \sigma_1) = \frac{2[A - B \cos 2(\alpha - \beta)] - 2\sigma_1 \tan \phi}{\tan \phi - \sqrt{1 + \tan^2 \phi}} \quad . \quad . \quad . \quad . \quad . \quad . \quad . \quad . \quad . \quad . \quad . \quad . \quad . \quad [23]$$

The constants A and B may be determined in the following manner. Note that at $\beta = \alpha$, $\cos 2(\alpha - \beta) = 1$, thus

$$\tau_o|_{\beta=\alpha} = A - B \ ,$$

and at $\beta = \alpha + 45°$, $\cos 2(\alpha - \beta) = 0$, thus

$$\tau_o|_{\beta=\alpha+45°} = A \ .$$

Therefore, if α is assumed to be 30°, then

$$\tau_o|_{\beta=75°} = A$$

and

$$\tau_o|_{\beta=75°} - \tau_o|_{\beta=30°} = B \ .$$

Therefore, to evaluate the continuously variable shear strength theory, it is necessary to run a series of compression tests at orientations of 30° and 75° (assuming $\alpha = 30°$) for various confining pressures, construct linear Mohr envelopes from the data, determine the values of τ_o and the average tan ϕ for the two orientations and then evaluate the constants A and B. Once A and B are known, the fracture strength of the material as a function of the orientation and the confining pressure can be calculated using equation [23].

If the assumption $\alpha = 30°$ is not made, it is necessary to run compressive strength tests for several pressures over the range of α from 20° to 50°, say at 5° or 10° intervals, to determine the actual value of α and then proceed as discussed to evaluate A and B.

In general it has been found[11] that equation [22] does not describe the actual variation of τ_o with respect to β over the entire range of β and usually predicts erroneous values of fracture strengths over the range of β from $0 \leq \beta \leq \alpha$.

Proposed Strength Criterion for Anisotropic Rock

The authors have noted that both the cohesive strength, τ_o, and the coefficient of internal friction, tan ϕ, may vary with respect to the orientation of the bedding or cleavage planes and the minimum principal stress for anisotropic rocks. This leads the authors to speculate that the general form of a fracture criterion for anisotropic rock, based on the Mohr-Coulomb concepts, has the form

$$\tau = \tau_o\{\beta\} - \sigma \tan (\phi\{\beta\}) \ , \ . \ . \ . \ [24]$$

where $\tau_o\{\beta\}$ and tan $(\phi\{\beta\})$ represent the variation of τ_o and tan ϕ with respect to the orientation β and are determined experimentally.

The experimental evidence of this study indicates that the variation of τ_o relative to β is best described by

$$\tau_o = A_{1,2} - B_{1,2}[\cos 2(\alpha - \beta)]^n \ , \ . \ [25]$$

where A_1 and B_1 are constants that describe the behavior of τ_o over the range $0 \leq \beta \leq \alpha$ while the constants A_2 and B_2 describe the behavior over the range $\alpha < \beta \leq 90°$. The factor "n" is herein termed the "anisotropic type" factor and has the value 1 or 3 for rocks that have a "planar" type of anisotropy and a value of 5 or 6 or more for rocks that have a "linear" type of anisotropy.

Slates and shales that possess highly developed cleavage planes typify "planar" anisotropy while laminated or bedded rocks such as bedded sandstones or dolomites characterize "linear" anisotropy. The major petrographic difference between the two types of rocks, as visualized by the authors, is that the "planar" anisotropic rocks are composed of highly oriented tabular particles such as the micaceous minerals and are characterized by a regular planar parting which is independent of the bedding planes.[16] The "linear" anisotropic rocks are generally composed of particles that are usually angular in form and essentially isotropic in nature. The particles are segregated into layers or laminations that reflect the relative grain size of the particles, mineralogical content or the environment conditions of deposition.

In general, it could be said that "planar" anisotropic rocks derive their anisotropic behavior from the anisotropic nature of the "smallest" particle of the body itself, while "linear" anisotropic rocks derive their anisotropic behavior from the particular arrangement of particles that are in themselves essentially isotropic. Figure 2 shows the strength behavior as a function of orientation for a typical planar anisotropic rock and for a linear anisotropic rock. The data shown in Figure 2 is a part of the experimental data of this study which will be discussed in detail in a later section.

The planar anisotropy is illustrated by the fracture strength data for slate, while the Green River shale data (Green River shale is actually a highly laminated fine grain dolomite rock) illustrate the features of linear anisotropy quite well. In general, rocks that possess a linear anisotropy show a smaller degree of anisotropic strength behavior than the planar anisotropic rocks. That is to say that the ratio of the strength at the strongest orientation to the weakest orientation is less for linear anisotropic rocks than for planar anisotropic rocks. Also, the zone of anisotropic strength behavior, as a function of β, for linear anisotropic rocks is less than that of planar anisotropic rocks. Figure 2 illustrates this quite well. The zone of anisotropic behavior for the slate encompasses the entire range of β while that for Green River shale is confined to the range of β from 5° or 10° to 60° and above β = 60°, a strength "plateau" occurs. This strength plateau corresponds to the zone of isotropic failure of the material as predicted by both the Walsh-Brace theory and the single plane of weakness theory.

It has been noted both in this study and in the work done by Chenevert[12] that the variation of τ_o with respect to β is quite similar in form to that of the fracture strength. This is to be expected for any material that can be described by a "continuously variable shear strength" theory. Inspection of equation [23] indicates that it is the variance of τ_o with respect to β that controls or determines the nature of the fracture criterion with respect to the orientation of the anisotropy.

Figure 3 illustrates the relationship between β, τ_o, and n as calculated from equation [25] for various values of "n." In Figure 3, the constants $A_{1,2}$ and $B_{1,2}$ were chosen so as to hold the values of τ_o at 0° and 90° constant at 6000 psi and the value at 30° constant at 3000 psi as "n" was varied from 1 to 6. Figure 3 illustrates that as "n" is increased, the angular range or width of the anisotropic behavior of τ_o decreases and for values of "n" above 5, a "plateau" is generated over a range of β from 65° to 85° that closely approximates the 90° value or τ_o. When "n" is increased from 5 to 6, the length of the plateau is increased and the width of the zone of anisotropic behavior is decreased slightly. From the behavior of equation [25], as shown in Figure 3, it is apparent that values of "n" of 1 or 3 could be used to approximate the strength behavior of planar anisotropic rocks as a function of the orientation angle β, while the values of "n" of 5 or 6 or even greater generate curves that have the same characteristics as the strength behavior of linear anisotropic rocks.

It has also been noted in this study that tan ϕ may vary with respect to the orientation or may, for some rocks, be reasonably constant. The variance of tan ϕ is of the same nature as that of τ_o and can be described by the equation

$$\tan \phi = C_{1,2} - D_{1,2}[\cos 2(\alpha' - \beta)]^m \quad , [26]$$

where the constants C_1 and D_1 describe the behavior of tan ϕ over the range of $0° \leq \beta \leq \alpha'$ and C_2 and D_2 over the range $\alpha' < \beta \leq 90°$ and α' designates the orientation of the minimum value of tan ϕ.

It has been noted in both this study and the work done by Donath[13] that the orientation which gives the minimum value of tan ϕ may not necessarily be the same as the one for a minimum value of τ_o for planar anisotropic rocks. Donath observed that the orientation for the minimum value of tan ϕ for Martinsburg slate occurred at 45° while the slate tested in this study had a minimum tan ϕ at 50°. In both cases the minimum value of τ_o occurred at 30°. This phenomenon was not observed in the Green River shale data of this study. In one type of Green River shale (lean) tested, tan ϕ was observed to be essentially constant and in another series of tests on Green River shale (rich), the value of tan ϕ was found to vary according to equation [26] for m = 6 and α' = 30°. Chenevert[12] has noted that the value of α' for Arkansas sandstone, a fine grained laminated sandstone, is also 30°. From this information, it appears that the minimum value of tan ϕ and τ_o usually occur at the same orientation, $\alpha = \alpha' = 30°$, for linear anisotropic rocks while for planar anisotropic rocks, α' occurs around β = 45° as compared to β = 30° for α.

The fracture criterion for an anisotropic rock that has both a variable τ_o and tan ϕ can be found by combining equation [26] and [25] with equation [5].

$$(\sigma_3 - \sigma_1) = \frac{2\tau_o - 2\sigma_1 \tan \phi}{\tan \phi - \sqrt{\tan^2 \phi + 1}} \quad , \quad . \quad [27]$$

where

$$\tau_o = A_1 - B_1[\cos 2(\alpha - \beta)]^n$$

for $0° \leq \beta \leq \alpha$,

$$\tau_o = A_2 - B_2[\cos 2(\alpha - \beta)]^n$$

for $\alpha < \beta \leq 90°$, and

$$\tan \phi = C_1 - D_1[\cos 2(\alpha' - \beta)]^m$$

for $0 \leq \beta \leq \alpha'$,

$$\tan \phi = C_2 - D_2[\cos 2(\alpha' - \beta)]^m$$

for $\alpha' < \beta \leq 90°$.

The expressions for the variance of $\tan \phi$ and τ_o are purely empirical in nature and the constants A, B, C, and D must be determined from the experimental data. Figure 4 shows a plot of $\tan \phi/(\sqrt{\tan^2 \phi + 1} - \tan \phi)$ versus β for $\tan \phi = 0.800 - 0.400[\cos 2(\alpha' - \beta)]^m$ for $\alpha' = 45°$ and values of m = 1, 3, and 6. This plot illustrates the effect of a variable coefficient of internal friction, $\tan \phi$, on the fracture criterion. From Figure 4, it can be seen that the value of m = 1 produces a curve that closely resembles the strength behavior of planar anisotropic rocks while the higher values of m generate curves that more closely resemble the strength characteristics of linear anisotropic rocks.

The general form of the curves illustrated in Figure 3 and Figure 4, as well as the experimental data of this study, indicate that values of n of 1 or 3 and a value of m = 1 can be used, along with equations [25] and [26], to describe the behavior of τ_o and $\tan \phi$ for planar anisotropic rocks while values of n = 6 and m = 6 can be used to describe the variance of τ_o and $\tan \phi$ for the linear anisotropic rocks tested in this study.

To evaluate this proposed criterion it is necessary to run compressive strength tests at several pressures for orientations of β of 0°, 30°, and 90°, construct linear Mohr envelopes to obtain the values of τ_o and $\tan \phi$ for the orientations tested and then, using the appropriate anisotropy factors, determine the best set of empirical constants A, B, C, and D. Once A, B, C, and D have been determined, equation [27] can be used to predict the strength of the rock as a function of the orientation, β, and the confining pressure, σ_1. If the rock being tested possesses a "planar" type of anisotropy, then an additional orientation, say 45° or 50°, should be tested to determine whether the minimum value of $\tan \phi$ corresponds to that of τ_o.

EXPERIMENTAL STUDY

Compressive strength tests were run on cylindrical samples of three sedimentary, anisotropic rocks (a black slate and two types of Green River shale). The samples were tested over a confining pressure range from 1000 psi to 40,000 psi with the pore pressure held constant at atmospheric pressure. The orientation of the plane of anisotropy (bedding or cleavage plane) was varied between 0° and 90° relative to the applied axial load. For each test, the axial force applied to the specimen, the axial deformation of the specimen and the confining pressure were recorded as a function of time. The initial elastic strain rate of the sample was held constant for the duration of the tests on any given rock.

The basic data obtained were converted to stress-strain curves and the elastic modulus of each specimen tested was determined from the initial linear portion of the constructed stress-strain curves. The fracture strength or maximum strength of the samples were determined from the termination point or peak point of the derived stress-strain curves. In such a manner, the strength characteristics of the rocks studied, as a function of both the initial stress state, σ_1, and the orientation of the bedding or cleavage plane, were determined. Figure 5 shows a typical test specimen and illustrates the test parameters. For a detailed description of the experimental apparatus and procedure used in this study the reader should consult the literature.[11]

ROCK DESCRIPTIONS

Slate

The slate tested during this study was a fine grained, black slate. There were no discernible bedding planes within the material, but cleavage was well developed. The material was obtained from a building site on The University of Texas campus. Attempts to determine the exact geological age and formation of the source material were fruitless.

Green River Shale

Green River shale, commonly called Colorado Oil shale or just oil shale, is of Eocene age and outcrops in northeastern Utah, southwestern Wyoming, and northwestern Colorado. In actuality, it is neither a shale nor an oil-bearing rock in the usual sense of the word. It is composed of fine grained calcite and dolomite particles interbedded with a native, solid, high molecular weight, organic material called kerogen. The material is highly laminated in appearance and ranges in color from light gray or brown to dark brown. Upon retorting in the 700°-800°F range, Green River shale yields a synthetic crude oil of about 30° API.

The two types of Green River shale used in this study were highly distinctive in nature. The first type, called herein Green

River shale-1 (GRS-1), was quite competent mechanically and usually failed in a brittle (shear) manner over the pressure range studied. Samples of this material, upon retort, yielded 18-22 gallons of 30° API synthetic crude per ton of rock. Physically, the material was light brown to light gray in appearance and was highly laminated.

The second material, Green River shale-2 (GRS-2), was much darker in appearance and yielded 38-40 gallons of 30° API synthetic crude per ton of rock when retorted. Mechanically, the material behaved in a plastic manner over the pressure range studied and, as a rule, failed in shear only after considerable plastic strain.

Both types of Green River shale used in this study were obtained from the United States Bureau of Mines demonstration mine near Rifle, Colorado.

TEST RESULTS

Slate

Compressive strength tests on slate were run at confining pressures of 5000, 10,000, 15,000, 20,000, 25,000, 30,000, and 40,000 psi and orientation angles, β, ranging from 0° to 90° at 10° intervals. The compressive strength tests on slate, as shown in Figure 6, clearly show that planar anisotropy has a marked effect on the strength of the rock over the entire range of β and the pressure range studied. The general shape of the graphs of fracture strength versus orientation angle are concave upwards with minimum values of fracture strength occurring at β = 30° for the 5000 psi range and shifting uniformly to about 40° as the pressure is increased to 40,000 psi. The vertical line near the minimum fracture strength for each pressure curve shown in Figure 6 represents the locus of minimum strength values predicted by the proposed failure criterion.

The samples loaded parallel to the cleavage planes, β = 0°, sustained the highest level of differential stress before fracturing while the 90° orientation exhibited strengths that were from 6 to 18 percent lower than the 0° orientation. This behavior is opposite to that found by Donath[14] for Martinsburg slate, but agrees with data discussed by Jaeger in his discussion of Donath's paper.

The relative degree of anisotropic strength behavior for any given pressure is indicated by the anisotropy strength coefficient which is defined as the ratio of the strength at any particular orientation to the strength of the strongest orientation for a given confining pressure. The anisotropy strength coefficients for the slate studied appear in Table 1.

Inspection of the anisotropy strength coefficients indicates that as pressure increased, two phenomena occurred. The first is that the anisotropic behavior of the rock decreases. This is indicated by the increase in the value of the coefficients at β = 20° and 30° from 0.44 and 0.37 at 5000 psi to 0.63 and 0.49 at 40,000 psi. The second phenomenon is that the minimum value of the strength appears to have shifted to higher orientations and "levels out" over a wider range of orientations as the pressure increased. This feature is indicated by the coefficients at 30,000 and 40,000 psi for β = 30°, 40°, and 50° of 0.46, 0.46, 0.46, and 0.49, 0.48, 0.48 as compared to the coefficients at 5000 psi of 0.37, 0.44, and 0.52.

An explanation for the first phenomenon is not readily apparent, but one possible explanation is that as the material began to behave in a more "plastic" manner as the pressure increased, the anisotropic properties of the rock decreased. Similar results have been reported by Podio[17] who has noted that impact tests on Berea sandstone parallel and perpendicular to bedding planes gave markedly different results at low confining pressures, but quite similar results at higher values of confining pressure. The low pressure tests were characterized by brittle craters while the high pressure tests had "plastic" type craters.

The second phenomenon occurred as a result of the fact that the minimum value of the coefficient of internal friction, tan ϕ, occurred at an orientation of 50° as compared to an orientation of 30° for the minimum value of cohesive strength, τ_o. This created a situation where the failure envelopes actually intersected and the 40° to 50° orientations became "weaker" than the 30° orientation. Figure 7 illustrates this feature, and a Mohr stress circle drawn at the point of intersection of the 30°, 40°, and 50° envelopes indicates that the strength, of these orientations, at a confining pressure of approximately 20,000 psi should be equal. It is interesting to note that the anisotropy strength coefficients at 20,000 psi and at β = 30°, 40°, and 50° were 0.45, 0.44, and 0.44.

Linear Mohr envelopes were drawn for the orientations studied for all three rocks and the variance of τ_o and tan ϕ with respect to β was determined. These data were used to

evaluate the single plane of weakness theory and the proposed failure criterion. Figure 8 shows typical Mohr envelopes for the slate.

Figures 9 and 10 show the relationship between the fracture strength of slate and the confining pressure for eight of the ten orientations studied. Handin and Hager[18] have previously shown that the relationship between the maximum strength and confining pressure for several types of isotropic rocks is linear. As seen in Figures 9 and 10, this relationship is true also for slate up to pressures of about 20,000 psi where noticeable departure from linearity occurs on most of the curves. This compares nicely with a value of 1000 bars (14,500 psi) as reported by Donath for Martinsburg slate.

The stress-strain curves derived from the basic data were drawn and the elastic moduli were determined from the curves. Typical stress-strain curves for slate are shown in Figure 11. The points in black on the curves represent stress values associated with failure. The general types of failure modes noted for slate and the relative shape of the stress-strain curves associated with the mode of failure will be discussed in a latter section of this paper.

Green River Shale-1 (GRS-1)

Compressive strength tests on GRS-1 were run at confining pressures of 1000, 5000, 10,000, 15,000, and 25,000 psi and at orientations of 0°, 15°, 20°, 30°, 45°, 60°, 75°, and 90°. The fracture strength data for GRS-1 as a function of orientation are shown in Figure 12. The general shape of the curves in Figure 12 are quite different than those for slate. This difference illustrates quite well the behavior of a material that possesses a "linear" type anisotropy as compared to a planar type of anisotropy. The minimum values of strength, once again, occurred at $\beta = 30°$ and the maximum strength occurred at $\beta = 0°$. A strength "plateau" occurred over the range of β from 45° to 90°. This plateau represents the isotropic strength behavior where failure is controlled by the "short" crack system. The strength behavior over the range of β from 0° to 45° represents the zone where failure is controlled by the "long" crack system, that is to say, the anisotropic nature of the rock.

Figure 13 shows the relationship between the fracture strength and confining pressure for GRS-1, for five of the orientations studied. The strength-pressure curves were quite linear over the pressure range of 5000 to 15,000 psi and deviated slightly from linearity at 1000 psi and at 25,000 psi. The anisotropy strength coefficients for GRS-1 are given in Table 2. Inspection of the anisotropy strength coefficient for $\beta = 20°$, 20°, 30°, and 45° indicates that as the pressure increased the anisotropic behavior of the material decreased. This effect can be seen by comparing the values at 1000 psi and 25,000 psi. A log-log plot of the coefficients for $\beta = 30°$ and the confining pressure is reasonably linear and suggests that the anisotropic strength behavior of the material should disappear completely at a confining pressure of about 70,000 psi. The decrease in the anisotropic strength behavior can readily be seen by comparing the 25,000 psi curve in Figure 12 with the other confining pressure curves.

The relative degree of anisotropic strength behavior for GRS-1 was much less than that of the slate. The strength coefficients at 5000 psi and for $\beta = 30°$ are 0.44 for slate and 0.73 for GRS-1. Chenevert[12] reported a strength coefficient, at the same orientation and pressure, of about 0.77 for Arkansas sandstone, while Donath reported a coefficient of 0.17 for Martinsburg slate at similar conditions. From this limited information it appears that the planar anisotropic materials exhibit a higher degree of anisotropic strength behavior as compared to linear anisotropic rocks.

Typical stress-strain curves for the tests run on GRS-1 are shown in Figure 14. Figure 15 illustrates typical Mohr envelopes for GRS-1.

Green River Shale-2 (GRS-2)

Compression tests were run on GRS-2 at confining pressures of 1000, 5000, 10,000, 15,000, and 25,000 psi for orientations of 0°, 10°, 20°, 30°, 40°, 60°, and 90°. Mechanically, GRS-2 behaved in a plastic manner and shear faults were produced, as a rule, only after the material had suffered considerable plastic strain. As a result of this, the maximum strengths, determined from the stress-strain curves, as opposed to the fracture strengths, were used to study the strength characteristics of GRS-2 as a function of confining pressure and orientation. Figure 16 shows the variation in maximum strength as a function of the orientation for GRS-2 for the pressures studied. In general, the strength-orientation curves for GRS-2 are quite similar to those for GRS-1. The major differences are that the strength plateaus at the higher values of β are not as well developed and the anisotropic strength behavior of GRS-2 does not diminish as greatly as pressure is increased as was the case for GRS-1. The anisotropic

strength coefficients of GRS-2 for $\beta = 30°$ range from 0.61 at 1000 psi to 0.72 at 25,000 psi as compared to 0.63 to 0.90 for GRS-1. The anisotropic strength coefficients for GRS-2 are presented in Table 3.

The variance of the maximum strengths as a function of the confining pressure is shown in Figure 17. The maximum strength versus confining pressure curves, for all orientations studied, are remarkably linear over the 1000 to 15,000 psi confining pressure range and deviate from linearity only slightly at 25,000 psi. The slopes of these curves are similar for all orientations studied and are approximately one. The abnormally low values of the maximum strength versus confining pressure curves led the authors to speculate that since the samples were tested under closed piston conditions, the pore pressure of the samples might have increased in some fashion as the confining pressure increased. If such were the case, the maximum strengths noted would be lower than the true strengths for any particular orientation tested and the slopes of the strength versus pressure curves would be lower than the usual range of 2 to 4 for most rocks. Tests on a Green River shale having a comparable kerogen saturation have been performed by Heard[15] under both "closed" and "vented" piston conditions. These tests indicated that the pore pressure developed at confining pressures up to 3000 bars (43,500 psi) and at temperatures up to 300°C was negligible and had no effect on the strength of the material.

Typical stress-strain curves for the GRS-2 tests are shown in Figure 18, while typical Mohr envelopes are shown in Figure 19.

Comparison of Experimental Data to Theories

In order to compare the experimental data with the various theories discussed it was necessary to evaluate the coefficient of internal friction, tan ϕ, and the cohesive strength, τ_o, for each orientation and rock tested. To do this, linear Mohr envelopes were constructed for each orientation tested and the value of τ_o and tan ϕ were determined graphically. These parameters could also have been determined from the slopes and intercepts of the strength versus confining pressure curves.

Linear Mohr envelopes for two orientations, $\beta = 0°$ and 30°, for each rock tested are shown in Figures 8, 15, and 19. In general, it was found that the slate envelopes were essentially linear over the pressure range of 5000 to 20,000 psi and curvilinear at pressures above 25,000 psi. Both the GRS-1 and GRS-2 envelopes were essentially linear over the pressure range of 1000 to 15,000 psi and deviated slightly from linearity at 25,000 psi. The relative degree of the linear behavior of the Mohr envelopes as a function of pressure for each orientation and rock tested, is reflected in the range of linear behavior of the strength versus pressure curves as shown in Figures 9, 10, 13, and 17.

Table 4 lists the values of τ_o and tan ϕ. Figures 20, 21, and 22 show the variation of these two parameters with respect to the orientation and also the empirical relationships used to evaluate the proposed criterion (variable τ_o and tan ϕ criterion).

The friction coefficients, μ_s, μ_L, and the atmospheric strength values, C_{oL} and C_{os}, were determined from the slopes and intercepts of the 30° and 0° and 90° strength versus confining pressure curves and were used to evaluate the Walsh-Brace theory. Due to the fact that the Walsh-Brace theory and single plane of weakness theory are identical and the inherent disadvantageous of the continuously variable shear strength theory the experimental data was only compared with the Walsh-Brace theory and the variable τ_o and tan ϕ criterion.

Figures 23 and 24 show the slate data compared to the two theories for 5000, 10,000, and 20,000 psi confining pressure. For the three confining pressures shown in Figure 23, the variable τ_o and tan ϕ criterion fits the data quite well over the entire range of β. Above 20,000 psi, the criterion predicted values of strength that were much higher than those determined experimentally. This is a result of the fact that the linear Mohr envelopes used to describe the failure of the material at the lower pressures cannot be used to describe the strength of the material above the 20,000 to 25,000 psi level. Note in Figure 23 that the theory predicts a minimum strength orientation of about 32° at 5000 psi, 34° at 10,000 psi and 37° at 20,000 psi. The entire range of minimum strength orientations, as predicted by this theory, is shown in Figure 6. For the three pressures shown in Figure 24, the Walsh-Brace theory fits the data quite well over the orientation range of 0° to 40° or 50°, but begins to differ sharply at orientations above 50°. Recall that the Walsh-Brace theory and the single plane of weakness theory were developed to describe the strength behavior of rocks that can behave as either an isotropic or an anisotropic material, depending upon the orientation of the plane of anisotropy relative to the applied load. Thus, one should not expect these theories to describe the behavior of rocks, such as slate, that behave in an anisotropic manner at all

orientations. Once again, above 20,000 psi, the theory and experimental data did not agree.

The comparisons between the two failure criteria and the Green River shale data are shown in Figures 25 through 28. Both criteria describe the GRS-2 data quite well for all orientations and pressure studied but fail to describe the 25,000 psi data for GRS-1. Above 15,000 psi the Mohr envelopes for GRS-1 for nearly all orientations are nonlinear and thus the failure criteria fail.

It is interesting to note the range in the magnitude of the internal coefficient of friction, tan ϕ, presented in Table 4. The values of tan ϕ for slate ranged from 0.661 at $\beta = 0°$ to 0.268 at $\beta = 50°$ and back up to 0.500 at $\beta = 90°$. In the first case ($\beta = 0°$) failure occurred by shear across the cleavage planes. At this angle, the individual layers on each side of the fracture surface were oriented in such a manner that they interlocked as the fracture progressed, thus the relatively high value of friction. In the second case ($\beta = 50°$) shear occurred along the cleavage plane which also corresponds to the basal planes of the mica flakes within the slate. Basal planes contain directions of easy glide in mica and, thus, the friction at this orientation was understandably much lower. In the last case, fracture also occurred across the cleavage plane, but at this orientation the individual layers were oriented in such a manner that no interlocking of the layers occurred along the fracture. Thus, the friction should be higher than the 50° orientation because the failure surface was much rougher than the basal planes of the mica but lower than the 0° orientation, since no interlocking of layers occurred. Such was the case.

The values of tan ϕ for GRS-1 and GRS-2 ranged from 0.554 to 0.588 and 0.384 to 0.325, respectively. This small range of values seemed to indicate that individual grains that make up the Green River shale possessed no distinctive physical characteristics that influenced the anisotropic strength behavior of the material. Walsh and Brace contend that the friction coefficient μ_s (tan ϕ at $\beta = 0°$ and 90°) reflects the physical characteristics of the short Griffith "cracks" that are contained within the grain boundaries while μ_L (tan ϕ at $\beta = 30°$) reflects the long cracks that occur within the plane of anisotropy. Thus, it appears that the physical characteristics of the "long" and "short" crack systems for GRS are quite similar and probably differ only in that the "long" cracks are highly oriented, while the "short" cracks are randomly oriented.

Deformation Characteristics

Three types of failure were noted in the anisotropic rocks studied. These types are illustrated in Figure 29 and include shear faulting both across and along the bedding or cleavage plane; "plastic" flow or slip along the bedding or cleavage plane; and failure due to the formation of kink bands. The failure characteristics for all samples tested are presented in Tables 5 and 6.

All three types of failure were noted in the plate and GRS-2 samples. The type of failure was found to be both a function of the orientation and the confining pressure. For example, for slate, the 20,000 psi samples failed in shear at 0° and 90°, kinked at 10°, 20°, and 30°, and failed in a combination of plastic slip and shear faulting at 40° through 80°. An example of the effect of pressure on the failure mode is the 30° orientation for slate, failure occurred by shear faulting along the cleavage planes at 15,000 psi and below and by kinking above 15,000 psi.

The GRS-1 samples failed invariably by shear faulting at all pressures and orientations studied. At most orientations the 25,000 psi samples sustained some "plastic" deformation before faulting. It is conceivable that kinking or plastic slip might have occurred at higher pressures.

A detailed microscopic analysis of the deformation characteristics of the samples deformed during this study is currently under way. An attempt is being made to correlate the geometric features of the kink bands with the general stress fields associated with them and to determine what petrographic changes, if any, occurred within the deformation zones. The results of this study should be reported shortly by Budd.[19] From the data presented here, however, it is obvious that the failure mode of anisotropic rock is a function of both the confining pressure and the orientation of the anisotropy.

Orientation - Effect on Fault Angle

Figures 30 and 31 show the relationship between the fault angle, θ, and the orientation angle, β, for the three rocks studied. The fault angles for both GRS-1 and GRS-2 were influenced by the orientation of the bedding planes only over the range of β from about 20° to 45°. Fault angles across the bedding plane for GRS-1 ranged from 21° to 36° and averaged around 28°. The fault angles across the bedding plane for GRS-2 ranged from 24° to 36° and averaged around 30°. Griffith's theory

predicts failure angles that range from 30° at uniaxial compression to 45°, as the confining pressure increases. Experimental evidence indicates that the average failure angle does indeed vary over this range but that the average failure angle for most rocks, even at rather high values of confining pressure, is around 30°.

The orientation of the cleavage planes had a more pronounced effect on the fault angles for the slate tested as shown in Figure 31. The shear faults parallelled the cleavage planes over the range of β from 10° to 50°. The shear faults at 0° averaged around 15°, while the faults at orientation above 50° averaged around 42°. The 90° samples failed in a catastrophic manner and it was impossible to measure the fault angles. The results shown in Figure 31 are similar to those reported by Donath[14] for Martinsburg slate. Donath also reported that the shear faults at β = 90° ranged from around 25° to 35° and averaged about 30°. Donath concluded that shear fractures in slate were unaffected by the presence of the cleavage plane only at the orientation where the maximum compression was perpendicular to the cleavage. The data presented in Figure 31 tend to substantiate Donath's conclusion.

Variations in the Modulus of Elasticity

The modulus of elasticity was determined from the initial, linear part of the stress-strain curve for each sample tested. It was noted that the modulus of elasticity increased with increasing pressure for all three rocks, but there seemed to be no uniform relationship between the modulus and the orientation angle, β. Values of the modulus of elasticity ranged from 2.4×10^6 psi to 10.0×10^6 psi for slate with an average of 5.7×10^6 psi and from 2.2×10^6 psi to 4.5×10^6 psi for GRS-1 with an average of 3.2×10^6 psi. Values ranging from 0.6×10^6 psi to 2.0×10^6 psi were noted for GRS-2. The average for GRS-2 was 1.2×10^6 psi.

Figure 32 shows the variation of the average value of the modulus of elasticity as a function of confining pressure for each rock studied. In general, the value of the average modulus increased slightly with increasing confining pressure. The modulus for slate increased from 4.4×10^6 psi at 5000 psi to 7.0×10^6 psi at 40,000 psi, while the average modulus of GRS-1 increased from 2.6×10^6 at 1000 psi to 3.8×10^6 psi at 25,000 psi. The average values of the modulus for GRS-2 ranged from 1.0×10^6 psi at 1000 psi to 1.4×10^6 psi at 25,000 psi.

It was noted for several orientations (in particular 30°, 40°, 50°, 70°, and 90° for slate, 20° and 30° for GRS-1, and 60° for GRS-2) that the modulus of elasticity increased with confining pressure, reached a maximum value, and then decreased slightly with increasing pressure. This feature is illustrated in Figure 33 for one orientation for each rock tested. Brace[20] and Serafim[21] have reported that the modulus of elasticity for rocks such as granite, dolomite, quartzite and diabase also increased as pressure increased, but they noticed no peaking and subsequent decrease in the modulus over the pressure ranges studied. Simons[22] has reported that the dynamic modulus of elasticity for several shales not only increased with increasing confining pressures, but also increased with an increase in the rate of loading. Although Donath made no mention of the variation of the modulus of elasticity with respect to pressure, inspection of the graphical data presented in his paper indicates that the modulus of Martinsburg slate increased as the confining pressure increased up to a pressure of 1000 bars (17,400 psi) and then decreased in much the same manner as illustrated in Figure 33.

The moduli of elasticity were averaged for each orientation as well as for each pressure studied and the variations of the average modulus with respect to the orientation are shown in Figure 34. The data appear to indicate that, except for the slate, the plane of anisotropy has little or no influence on the modulus of elasticity. For the slate, the average modulus decreased from a value of 8.1×10^6 psi at 0° to 4.5×10^6 psi at 20° and then averaged about 4.8×10^6 psi from 20° to 80° and then increased to 7.5×10^6 psi at β = 90°.

The variation of the modulus for the Green River shale is not nearly so pronounced as that of the slate. The values for GRS-1 ranged from 3.6×10^6 psi at β = 0° to 2.8×10^6 psi at β = 90° and averaged about 3.2×10^6 psi, while the modulus of GRS-2 ranged from 1.7×10^6 psi at β = 0° to 0.9×10^6 psi at β = 30° and back up to 1.2×10^6 psi at β = 90°. The average value for GRS-2 was about 1.2×10^6 psi.

TENSILE STRENGTH TESTS

The tensile strength of brittle polycrystalline materials has proved to be a difficult parameter to measure. Several techniques have been employed to determine the tensile strength of rocks, but none have been found to be totally satisfactory. The standard uniaxial tension test is perhaps the most common technique employed, but it too has its faults. Small misalignments in the sample and stressing

apparatus generate bending moments that lower the measured strength. Also, additional problems arise from the gripping technique used and premature failure often occurs due to stress concentrations induced by gripping.

A technique commonly used to determine the tensile strength of rocks is the bending test. In this test, a beam specimen of rock is strained by bending and tensile stresses have developed on the convex side of the beam. If the rock behaves as an elastic body--if the behavior of the rock in compression is the same as that in tension--and if there are no surface scratches present, then the bending moment at failure is a measure of the tensile strength of the material.

Another indirect testing method that is rapidly gaining acceptance in testing laboratories is the diametral compression or "Brazilian" test. In this test, a thin circular disk is loaded along a diameter between the platens of a compression testing machine. This method of loading develops a tensile stress that is perpendicular to the loading axis. Tensile failure of the specimen occurs by splitting along the loading axes and the load at failure is used to calculate the tensile strength. The major fault of this technique is its inadaptability to certain materials. High shear stresses are developed in the material adjacent to the loading platens and many materials fail prematurely due to shear.

The Brazilian test technique was chosen to study the tensile strength behavior of the anisotropic rocks tested during this study. This technique was chosen because of the simplicity of the test itself and because the failure surface is predetermined thus enabling the effect of bedding planes on tensile strength to be studied.

It was found that only the GRS-1 material was suitable for this type of testing. The slate failed prematurely in "brittle" shear at all orientations tested and the GRS-2 deformed appreciably in a plastic manner before failing in shear. Tensile tests on GRS-1 were performed at orientations of 0°, 30°, 45°, 60°, 75°, and 90° (the orientation angle in this case is measured between the bedding plane and σ_1) at atmospheric pressure and at 0° at 2500 psi.

Tensile Strength Criterion

Walsh and Brace have modified Griffith's theory of tensile failure so that it applies to anisotropic material. Their analysis states that the tensile strength of the material is affected only by the anisotropic nature of the material over a certain range of β and by letting K be equal to the tensile strength at 90°, $T_{o\ell}$, the anisotropic strength behavior is given by

$$T = \frac{2T_{o\ell}}{\sin\beta(1 + \sin\beta)} \quad \ldots\ldots [28]$$

The tensile strength in the range of β where failure is controlled by the short cracks is given by

$$T = T_{os} \quad \ldots\ldots\ldots [29]$$

where T_{os} is the maximum tensile strength of the material (the maximum usually occurs at $\beta = 0°$).

To evaluate the Walsh-Brace theory, it is necessary to determine the tensile strength at two orientations, 0° and 90°. One then evaluates equations [28] and [29] and use the smaller value as the tensile strength for the particular orientation in question.

Brazilian Test

In the Brazilian test, a right circular disk is compressed diametrally between two flat steel pistons. If the behavior of the material is essentially elastic and the load is confined to a line along the periphery of the sample, then the theory[23,24] predicts a constant tensile stress along the loaded diameter that is normal to the applied load. The tensile strength at failure is given by

$$\sigma_1 = T = \frac{2F}{\pi tD}, \qquad [30]$$

where

σ_1, T = tensile strength at failure ($lb/in.^2$),
F = applied load (lb),
t = thickness of the disk (in.),
D = diameter of the disk (in.).

In practice it is almost impossible to achieve a perfect line load and in most cases it is not desirable to do so. It has been found by several investigators that if a small amount of padding material is placed between the steel piston and the sample, more reliable and consistent tensile strengths are generated. This in effect widens the load area and creates what has been termed "strip" loading. By strip loading the sample, the compressive and shear stresses in the sample near the loaded area are reduced considerably. Thus, premature failure by shear, in many cases, is avoided. Figure 35 shows a typical strip loaded disk sample and illustrates the notation used.

Hondros[25] has analyzed the stress distribution in a thin disk loaded by "strip loading." He found that the stresses of interest in the Brazilian test--that is, the stresses acting along the failure plane--are given by

$$\sigma_{\theta Y} = \frac{2F}{a\pi t}\left[\frac{(1 - r^2/R^2)\sin 2\rho}{1 - 2r^2/R^2 \cos 2\rho + r^4/R^4} - \tan^{-1}\left(\frac{1 + r^2/R^2}{1 - r^2/R^2}\right)\tan\rho\right], \quad [31]$$

$$\sigma_{rY} = -\frac{2F}{a\pi t}\left[\frac{(1 - r^2/R^2)\sin 2\rho}{1 - 2r^2/R^2 \cos 2\rho + r^4/R^4} + \tan^{-1}\left(\frac{1 + r^2/R^2}{1 - r^2/R^2}\right)\tan\rho\right], \quad [32]$$

where

$\sigma_{\theta Y}$ = tangential normal stress along Y-Y′,
σ_{rY} = radial normal stress along Y-Y′,
F = applied load,
a = projected width of the load section,
t = thickness,
ρ = load angle,
r = radial distance to a point from the center of the disk,
R = radius of the disk.

Figure 36 shows the variation of the stresses $\sigma_{\theta Y}$ and σ_{rY} along the loaded diameter Y-Y′ for the case of $2F/(a\pi t) = 1$ and $\rho = \tan^{-1}(1/12)$.

The tensile stress at the center of the disk can be found from equation [31] by letting r = 0;

$$\sigma_{\theta Y} = \frac{2F}{a\pi t}[\sin 2\rho - \rho] \quad [33]$$

For small values of ρ, $\sin 2\rho \cong 2\rho$ and $\sin\rho = (a/2)/(D/2) = a/D \cong \rho$, thus equation [33] reduces to

$$\sigma_{\theta Y} \cong \frac{2F}{\pi t D}. \quad [34]$$

From this development, it can be seen that for small values of ρ, the stresses at the center of the disk with strip loading is the same as in the case with line loading. Inspection of Figure 36 shows that the tensile stress, $\sigma_{\theta Y}$, is essentially constant over 75 percent of the diameter and is equivalent to the stress at the center of the disk. Strip angles of $\rho = \tan^{-1}(1/12)$ and $\rho = \tan^{-1}(1/6)$ were used in this study and the percent error between equations [34] and [30] are 1 percent and 3 percent, respectively.

Fairhurst[26] has recently analyzed the validity of the Brazilian test. He modified Griffith's criterion to account for variable ratios of compressive strength to tensile strength and used this criterion as the basis of failure. Fairhurst studied the cases of $\rho = \tan^{-1}(1/12)$ and $\rho = \tan^{-1}(1/6)$ for compressive-tensile strength ratios, n, of 8, 10, and 12 and concluded that for values of n less than 12, the tensile strengths predicted by the Brazilian test technique, using a strip angle of $\rho = \tan^{-1}(1/12)$, could be as much as 30 percent low. Fairhurst found that for $n > 12$, the $\rho = \tan^{-1}(1/12)$ strip load case predicted tensile strengths that were more representative of tensile failure along the entire loaded diameter rather than a small part in the vicinity of the center of the disk. He found that the same thing applied to the $\rho = \tan^{-1}(1/6)$ case for all values of n studied.

Based on the compressive strengths determined from the strength-pressure curves, the compressive-tensile strength ratios for GRS-1 ranges from 30 to 90° to 6.8 at 30° and back up to 11 at 0°. Both strip angles studied by Fairhurst, $\rho = \tan^{-1}(1/12)$ and $\rho = \tan^{-1}(1/6)$, were used in this study for the atmospheric tensile tests and the results were comparable at all orientations tested.

As previously mentioned, Brazilian tests were also run at a confining pressure of 2500 psi for the 0° orientation. The effect of the confining pressure on the test sample consisted simply of superposing a uniform hydrostatic stress state on the sample. The tensile strength for this case is given by

$$T = -P + \frac{2F}{\pi t D}, \quad [35]$$

where P is the confining pressure in psi.

Experimental Results

The tensile strengths as determined from the Brazilian tests are presented in Table 7. The average tensile strengths ranged from 3077 psi at 0° to 1017 psi at 90°. The average tensile strengths along with the range of the strengths noted as a function of β are shown in Figure 37. As seen in Figure 37, the tensile strength of GRS-1 is highly dependent upon the orientation of the bedding planes and this variance is described remarkably well by the modified Griffith theory.

Hobbs[8] has reported the results of tensile tests run on six laminated rocks (siltstones, sandstones, and a mudstone). His results are similar to the results of the tests on GRS-1. Inspection of the data

presented by Hobbs indicated that the tensile strength behavior of two of the rocks (both siltstones) could be described by the modified Griffith theory.

The typical failure modes observed in the Brazilian tests on GRS-1 are shown in Figure 38. In general, the plane of fracture was reasonably linear and occurred along the loaded diameter. In several cases, as indicated by the 0°, 45°, and 90° orientations in Figure 38, two tensile failure surfaces were generated. The 30° orientation sample illustrates another type of tensile failure that has been termed "triple cleft" failure by Chenevert. A few samples failed in shear. Shear failures were readily noticeable as the samples failed into many parts and there were no distinct tensile failure planes. The tensile strength of all samples that failed in shear were rejected from the analysis of the data. Out of a total of 28 tests, only three failed in shear.

The average tensile strength of the samples tested at a confining pressure of 2500 psi and at $\beta = 0°$ was 3040 psi. This compares nicely with the average value of 3077 psi for the atmospheric tests and indicates that the tensile strength is independent of pressure. Heard[15] has run tensile tests on Solenhofen limestone (using the Brazilian test technique) at pressures up to 8 kilobars (116,000 psi). He found that the tensile strength increased at a rate of 0.011 psi per psi of confining pressure up to 5 kilobars. Above 5 kilobars, the rock became ductile and the data became meaningless. This illustrates the relatively insignificant effect that pressure has on the tensile strength of rocks.

CONCLUSIONS

Based on the analysis of the current fracture criteria for anisotropic rocks and the experimental program presented in this paper, the following conclusions may be drawn.

1. The Walsh-Brace theory and Jaeger's single plane of weakness theory are identical.

2. The Walsh-Brace theory is best suited to describe the fracture strength of anisotropic rocks characterized by bedding planes.

3. The proposed variable τ_o and tan ϕ criterion can be used to describe the fracture strength of anisotropic rock characterized by bedding planes or cleavage planes.

4. All theories discussed can only be applied to anisotropic rocks that have linear Mohr envelopes.

5. The compressive strength behavior of anisotropic rocks is a function of both the confining pressure and the orientation of the bedding or cleavage plane to the applied stress. The minimum compressive strength usually occurred at an orientation of 30°, while the maximum strength occurred at 0°.

6. The anisotropic strength behavior of the rocks tested, as indicated by the anisotropic strength coefficients for any given orientation, tends to decrease as pressure increases.

7. The cohesive strength, τ_o, and the coefficient of internal friction, tan ϕ, vary with the orientation of the plane of anisotropy and the nature of this variation is a function of the type of anisotropy.

8. The failure behavior of both types of Green River shale tested in this study may be described by the Walsh-Brace theory or by the variable τ_o and tan ϕ criterion.

9. The failure behavior of the slate tested in this study could only be described satisfactorily by the variable τ_o and tan ϕ criterion.

10. The average modulus of elasticity for the anisotropic rocks tested increased with increasing confining pressure. There appeared, however, to be no systematic relationship between the modulus of elasticity and the orientation of the sample.

11. Anisotropic rocks fail by (1) shear faulting across the plane of anisotropy or shear faulting along the plane of anisotropy, (2) plastic flow or slip along the plane of anisotropy, or (3) kinking. The exact nature of the failure is dependent upon the confining pressure and the orientation of the sample.

12. The Brazilian test technique can be used to determine the tensile strength behavior of anisotropic rocks and has distinct advantages over the uniaxial tension test technique.

13. The tensile strength variation of Green River shale is a function of the orientation. The minimum tensile strength occurred when bedding planes of the specimen were oriented at 90° to the induced tensile stress, while the maximum strength occurred at the 0° orientation.

14. The variance of the tensile strength with respect to the orientation of the bedding planes for Green River shale can be described by the modified Griffith theory.

15. The tensile strength of Green River shale at the 0° orientation appears to be insensitive to confining pressure.

ACKNOWLEDGMENTS

Financial support of this work by the Texas Petroleum Research Committee, the University Research Institute of The University of Texas and the American Petroleum Institute is gratefully acknowledged. Also, the authors wish to acknowledge Shell Development Company for releasing the design plans from which the equipment used in this study was built. Thanks are due to students Augusto Podio, J. Yang, Clifford Budd and Fred Brown for assistance at various times. Finally, the authors wish to thank Dr. Carl Gatlin for his stimulating ideas during the formulation of this project.

REFERENCES

1. Jaeger, J. C.: "Shear Failure of Anisotropic Rocks", Geol. Mag. [1960] 97, 65-72.
2. Walsh, J. B. and Brace, W. F.: "A Fracture Criterion for Brittle Anisotropic Rock", Jour. Geophys. Res. [1964] 69, No. 16, 3449-3456.
3. McClintock, F. A. and Walsh, J. B.: "Friction on Griffith Cracks in Rocks under Pressure", Proc. Fourth U.S. Natl. Cong. Appl. Mech. [1963] 1015.
4. Griffith, A. A.: "Theory of Rupture", Proc. First Internatl. Cong. Appl. Mech. [1924] 55-63.
5. Hoek, E.: "Symposium on Strata Control and Rock Mechanics", Johannesburg, South Africa [May 22, 1964].
6. Brace, W. F.: "An Extension of the Griffith Theory of Fracture to Rocks", Jour. Geophys. Res. [1960] 65, No. 10, 3477-3480.
7. Jaeger, J. C.: Elasticity, Fracture and Flow, John Wiley and Sons, Inc., New York [1962].
8. Sykes, R.: Unpublished rock mechanics laboratory data, The Univ. Texas [1966].
9. Gnirk, P. F. and Cheatham, J. B.: "An Experimental Study of Single Bit-Tooth Penetration into Dry Rock at Confining Pressures of 0 to 5,000 psi", Second Conf. on Drilling and Rock Mech., The Univ. Texas [1965].
10. Wuerker, R. G.: "Annotated Tables of Strength and Elastic Properties of Rocks", AIME Pet. Branch, Paper 663 G [1956].
11. McLamore, R. T.: "Strength Deformation Characteristics of Anisotropic Rocks", Ph.D. Dissertation, The Univ. Texas [1966].
12. Chenevert, M. E.: "The Deformation-Failure Characteristics of Laminated Sedimentary Rocks", Ph.D. Dissertation, The Univ. Texas [1964].
13. Donath, F. A.: "Experimental Study of Shear Failure in Anisotropic Rocks", Geol. Soc. Am. Bull. [1961] 72, 985.
14. Donath, F. A.: "Strength Variation and Deformational Behavior in Anisotropic Rocks", State of Stress in the Earth's Crust, American Elsevier Publishing Co., New York [1964] 281.
15. Heard, H. C.: Personal Communication.
16. Turner, F. J. and Weiss, L. E.: Structural Analysis of Metamorphic Tectonites, McGraw-Hill Book Co., Inc., New York [1963].
17. Podio, A. L.: "Effect of Pore Fluid Viscosity during Single Blow Chisel Impact", M.S. Thesis, The Univ. Texas [1965] 44.
18. Handin, J. and Hager, R. V.: "Experimental Deformation of Sedimentary Rocks under Confining Pressure; Tests at Room Temperature on Dry Samples", Bull. Am. Assoc. Pet. Geol. [1957] 41, 1-50.
19. Budd, C.: "A Microscopic Examination of Mechanically Deformed Anisotropic Sedimentary Rocks", M.S. Thesis in Progress, The Univ. Texas.
20. Brace, W. F.: "Brittle Fracture of Rocks", State of Stress in the Earth's Crust, American Elsevier Publishing Co., New York [1964] 111.
21. Serafim, J. L.: "Rock Mechanics Considerations in the Design of Concrete Dams", State of Stress in the Earth's Crust, American Elsevier Publishing Co., New York [1964] 611.
22. Simons, L. H.: "Elastic Properties of Shales", First Conf. on Drilling and Rock Mech., The Univ. Texas [1963].
23. Timoshenko, S. and Goodier, J. N.: Theory of Elasticity, McGraw-Hill Book Co., Inc., New York [1951].
24. Frocht, M. M.: Photoelasticity, Vol. II, John Wiley and Sons, Inc., New York [1948] 125.
25. Hondros, G.: "The Evaluation of Poisson's Ratio and the Modulus of Materials of a Low Tensile Resistance by the Brazilian (Indirect Tensile) Test with Particular Reference to Concrete", Australian Jour. Appl. Sci. [1959] 10, No. 3, 243-268.
26. Fairhurst, C.: "On the Validity of the Brazilian Test for Brittle Materials", Internatl. Jour. Rock Mech. and Mining Sci. [1964] 1, 535-546.

Table 1

ANISOTROPY STRENGTH COEFFICIENTS FOR SLATE

Confining Pressure (psi)	Orientation Angle, β									
	0°	10°	20°	30°	40°	50°	60°	70°	80°	90°
5,000	1.00	0.77	0.44	0.37	0.44	0.52	0.61	0.74	0.88	0.94
10,000	1.00	0.75	0.48	0.36	0.42	0.45	0.56	0.66	0.72	0.85
15,000	1.00	0.76	0.50	0.38	0.42	0.42	0.53	0.64	0.74	0.84
20,000	1.00	0.77	0.53	0.45	0.44	0.44	0.58	0.70	0.78	0.87
25,000	1.00	0.75	0.58	0.42	0.43	0.43	0.57	----	0.74	0.82
30,000	1.00	0.75	0.59	0.46	0.46	0.46	0.59	0.69	0.78	0.84
40,000	1.00	0.75	0.63	0.49	0.48	0.48	0.60	0.72	----	0.88
Average	1.00	0.76	0.54	0.42	0.43	0.46	0.58	0.69	0.77	0.86

Table 2

ANISOTROPY STRENGTH COEFFICIENTS FOR GRS-1

Confining Pressure psi	Orientation Angle, β							
	0°	15°	20°	30°	45°	60°	75°	90°
1,000	1.00	0.81	0.77	0.63	0.86	0.88	0.85	0.91
5,000	1.00	0.92	0.82	0.73	0.86	0.86	0.88	0.93
10,000	1.00	0.95	0.89	0.81	0.91	0.95	0.95	0.97
15,000	1.00	0.96	0.92	0.85	0.95	0.94	0.96	0.97
25,000	1.00	0.94	0.93	0.90	0.91	0.99	0.95	0.96
Average	1.00	0.92	0.86	0.78	0.90	0.92	0.92	0.95

Table 3

ANISOTROPIC STRENGTH COEFFICIENTS FOR GRS-2

Confining Pressure psi	Orientation Angle β						
	0°	10°	20°	30°	40°	60°	90°
1,000	1.00	0.89	0.73	0.61	0.67	0.80	0.86
5,000	1.00	0.91	0.80	0.67	0.73	0.85	0.91
10,000	1.00	0.92	0.80	0.68	0.74	0.86	0.90
15,000	1.00	0.93	0.83	0.69	0.76	0.86	0.90
25,000	1.00	0.90	0.84	0.72	0.78	0.84	0.91
Average	1.00	0.91	0.80	0.67	0.74	0.84	0.90

Table 4

VALUES OF COHESIVE STRENGTH, τ_o, AND THE COEFFICIENT OF INTERNAL FRICTION, tan ϕ

SLATE		
β (degrees)	τ_o (psi)	tan ϕ
0	8,800	0.661
10	7,500	0.544
20	4,200	0.466
30	3,800	0.384
40	5,100	0.344
50	7,600	0.268
60	7,800	0.364
70	9,300	0.414
90	10,200	0.509

GRS-1		
β (degrees)	τ_o (psi)	ϕ
0	10,600	29°
15	9,000	30°
20	7,800	30°
30	6,400	30.5°
45	8,100	30.5°
60	8,600	30°
75	8,600	30.5°
90	9,100	30.5°

GRS-2		
β (degrees)	τ_o (psi)	tan ϕ
0	6,600	0.384
10	6,000	0.374
20	5,000	0.361
30	4,200	0.325
40	4,600	0.344
60	5,300	0.376
90	5,600	0.378

Table 5

DEFORMATION MODES FOR SLATE*

Confining Pressure psi	Orientation Angle, β									
	0°	10°	20°	30°	40°	50°	60°	70°	80°	90°
5,000	SAC	SAL	SAL	SAL	SAL	SAL	SAC	SAC	SAC	SAC
10,000	SAC	SAL	SAL	SAL	SAL	SAL	SAC	SAC	SAC	SAC
15,000	SAC	K	K	SAL	SAL	PS / SAL	PS / SAL	PS / SAC	SAC	SAC
20,000	SAC	K	K	K	PS / SAL	PS / SAL	PS / SAL	PS / SAC	PS / SAC	SAC
25,000	K / SAC	K	K	K	PS / SAL	PS	PS	PS	PS / SAC	SAC
30,000	K / SAC	?	K	K	PS	PS	PS	PS	PS / SAC	SAC
40,000	K / SAC	K	K	K	PS	PS	PS	PS	SAC	SAC

* SAC - Shear Across Cleavage Plane
SAL - Shear Along Cleavage Plane
K - Kinking
PS - Plastic Slip

Table 6

DEFORMATION MODES FOR GREEN RIVER SHALE*

Confining Pressure psi	Orientation Angle, β, Degrees, GRS-1							
	0°	15°	20°	30°	45°	60°	75°	90°
1,000	SAC	SAL	SAL	SAL	SAC	SAC	SAC	SAC
5,000	SAC	SAC / SAL	SAL	SAL	SAL / SAC	SAC	SAC	SAC
10,000	SAC	SAC	SAL / SAC	SAL	SAL / SAC	SAC	SAC	SAC
15,000	SAC	SAC	SAL	SAL	SAC	SAC	SAC	SAC
25,000	SAC	SAC	SAL	SAL	SAC	SAC	SAC	SAC

	Orientation Angle, β, Degrees, GRS-2						
	0°	10°	20°	30°	40°	60°	90°
1,000	SAC	SAC	SAC	SAL	SAL	SAC	SAC
5,000	SAC	SAC	PS / SAC	SAL	SAL	SAC	SAC
10,000	SAC	K / SAC	K	SAL / PS	SAL / PS	SAC / SAL	SAC
15,000	K / SAC	K	K	SAL	PS / SAL	PS / SAL	SAC
25,000	K	K	K	PS	PS K	SAC	SAC

*SAC - Shear Across Bedding
SAL - Shear Along Bedding
K - Kinking
PS - Plastic Slip

Table 7

TENSILE STRENGTHS OF GREEN RIVER SHALE-1

β, Angle Between σ_1 and Bedding Plane (degrees)	Tensile Strength (psi)	Average Tensile Strength (psi)	Confining Pressure (psi)	X $\rho=\tan^{-1}(x)$
0	3141		0	(1/6)
0	2904	3077	0	(1/6)
0	3186		0	(1/12)
30	2763		0	(1/12)
30	2915	2848	0	(1/6)
30	2895		0	(1/12)
30	2817		0	(1/6)
45	1758		0	(1/6)
45	1674	1693	0	(1/12)
45	1648		0	(1/6)
60	1372		0	(1/12)
60	1285	1342	0	(1/6)
60	1333		0	(1/12)
60	1377		0	(1/6)
75	1106		0	(1/6)
75	1211	1133	0	(1/12)
75	1056		0	(1/6)
75	1160		0	(1/12)
90	950		0	(1/12)
90	1058	1017	0	(1/12)
90	1043		0	(1/6)
0	2974		2500	(1/6)
0	3008	3040	2500	(1/6)
0	3140		2500	(1/6)
0	3040		2500	(1/6)

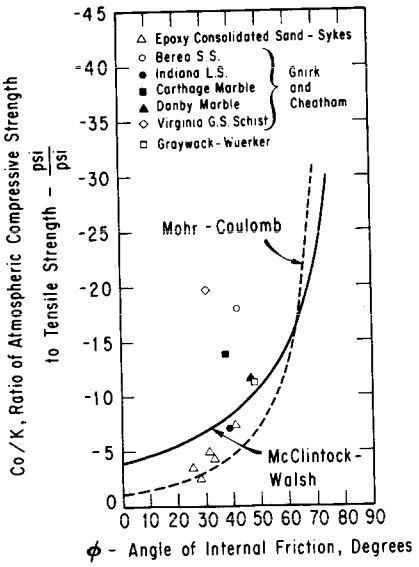

Fig. 1. Relationship Between Co/K and ϕ

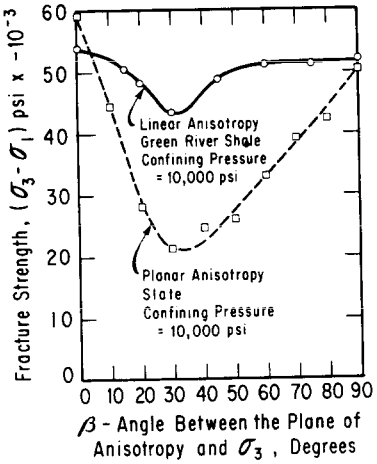

Fig. 2. Typical Strength Variation of Planar and Linear Anisotropic Rocks as a Function of Orientation

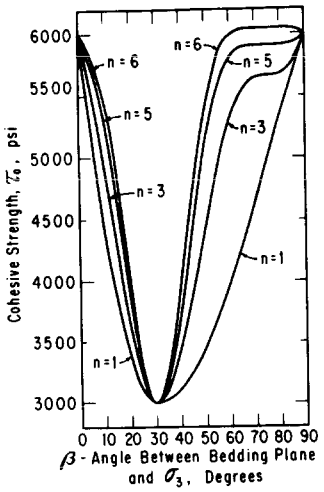

Fig. 3. Cohesive Strength vs. β for Various Values of "n"

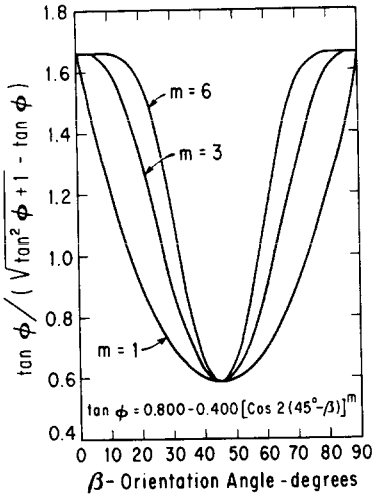

Fig. 4. Variation of $\tan\phi / \sqrt{\tan^2\phi + 1} - \tan\phi$ as a function of β.

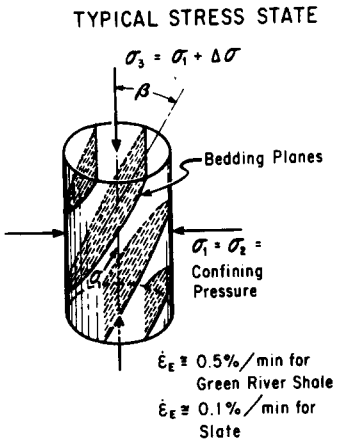

Fig. 5. View of Typical Sample Showing Parameters (β, σ and $\dot{\varepsilon}_E$) Varied During Testing

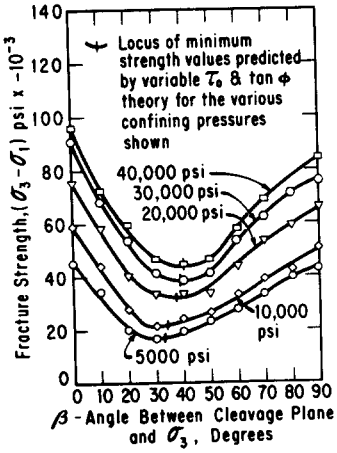

Fig. 6. Fracture Strength vs. Orientation Angle β for Slate at Various Confining Pressures

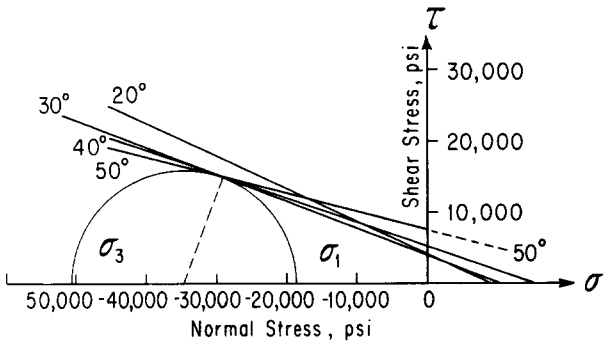

Fig. 7. **Failure Envelopes at Various Orientations of β for Slate**

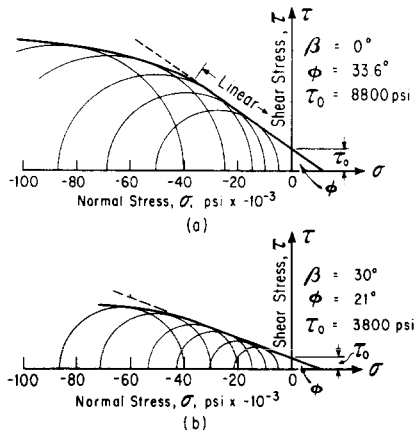

Fig. 8. **Typical Failure Envelopes for Slate**

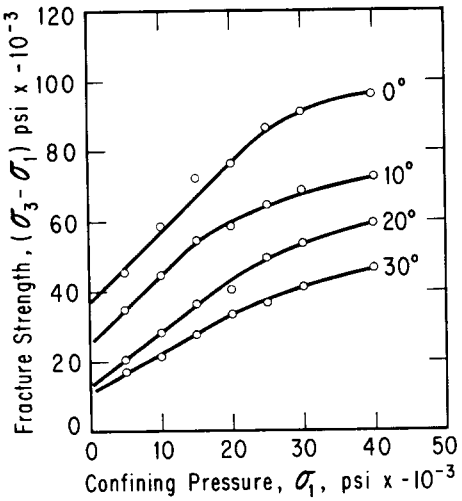

Fig. 9. **Fracture Strength Versus Confining Pressure for Slate at Various Orientations**

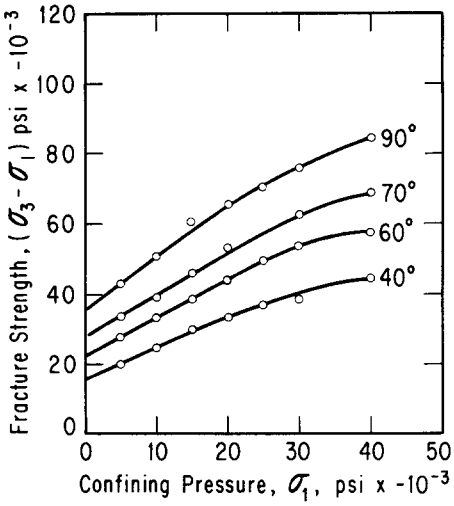

Fig. 10. **Fracture Strength Versus Confining Pressure for Slate at Various Orientations**

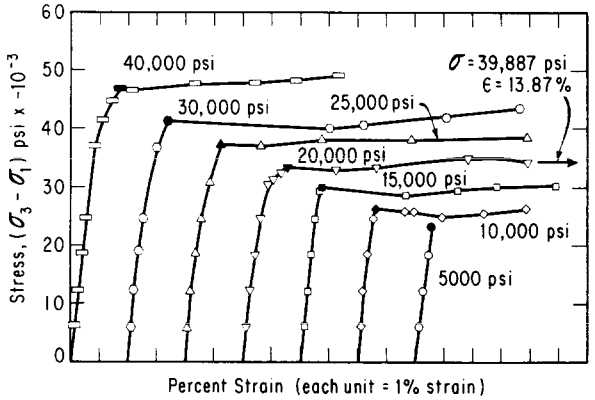

Fig. 11. Stress-Strain Curves for Slate at Various Confining Pressures, $\beta = 50°$

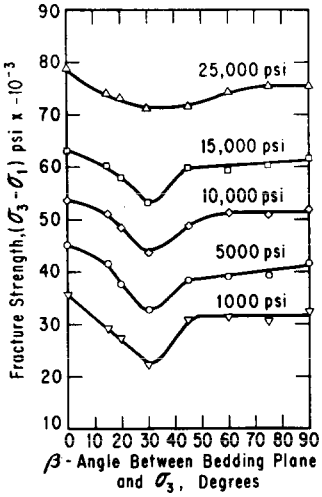

Fig. 12. Green River Shale-1 Fracture Strength Data

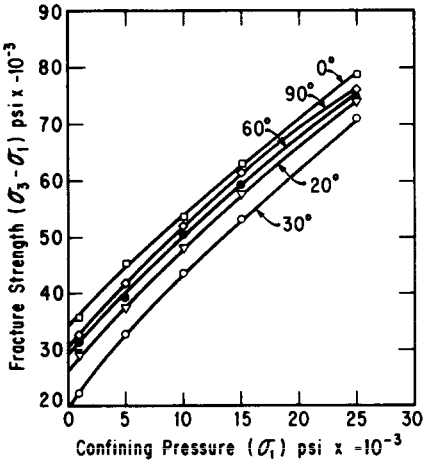

Fig. 13. Fracture Strength vs. Confining Pressure for Green River Shale - 1 at Various Orientations

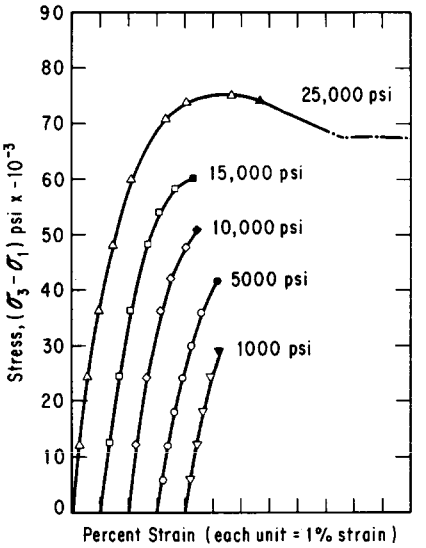

Fig. 14. Stress-Strain Curves for Green River Shale - 1 at Various Confining Pressures, $\beta = 15°$

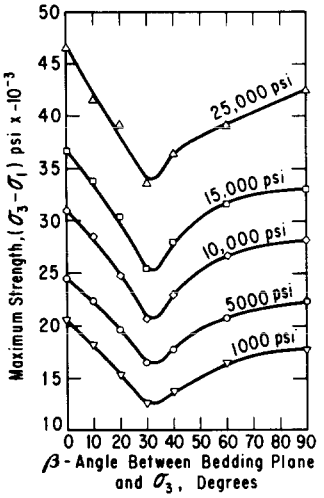

Fig. 16. Green River Shale - 2 Maximum Strength Data

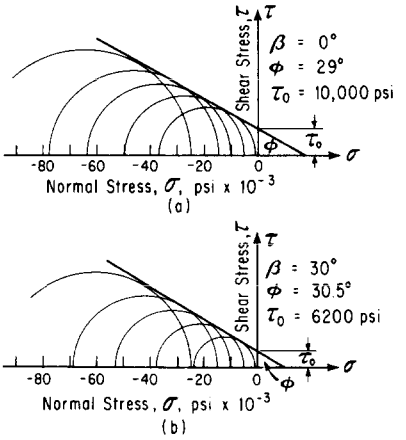

Fig. 15. Typical Failure Envelopes for Green River Shale - 1

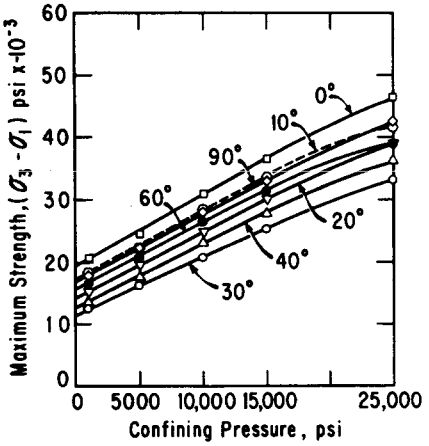

Fig. 17. Maximum Strength vs. Confining Pressure for Green River Shale - 2

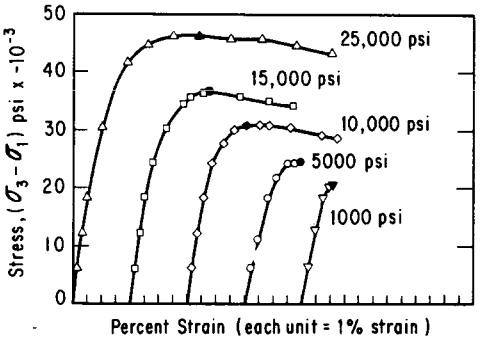

Fig. 18. Stress-Strain Curves for Green River Shale - 2 at Various Confining Pressures, $\beta = 0°$

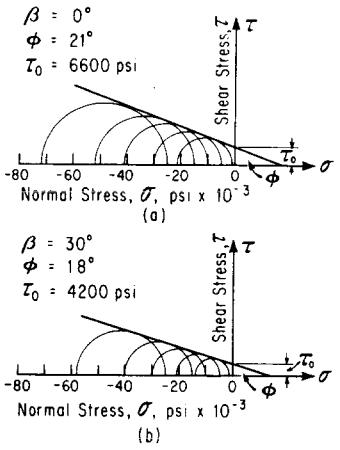

Fig. 19. Typical Failure Envelopes for Green River Shale - 2

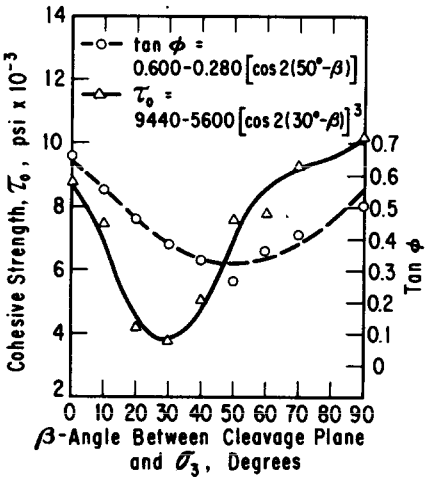

Fig. 20. Variation of τ_0 and tan ϕ with respect to β for Slate

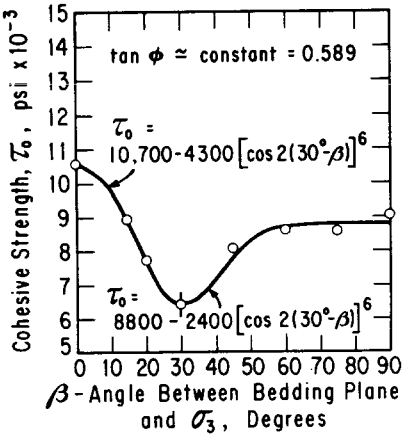

Fig. 21. Variation of τ_0 with respect to β for Green River Shale - 1

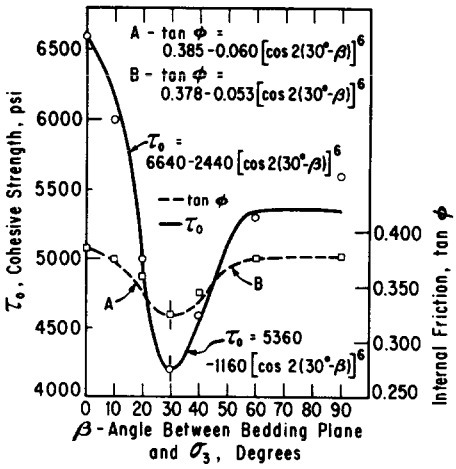

Fig. 22. Variance of τ_0 and tan ϕ with respect to β for Green River Shale - 2

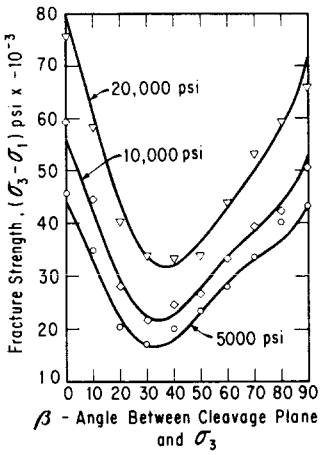

Fig. 23. Comparison of Variable τ_0 and tan ϕ Criteria with the Experimental Slate Data

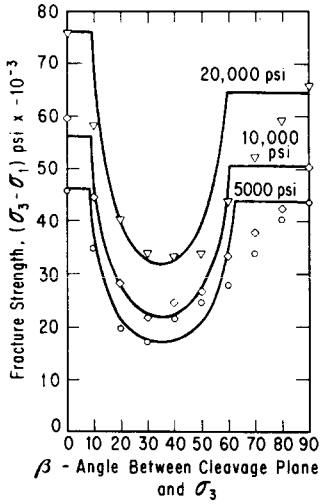

Fig. 24. Comparison of the Walsh - Brace Theory with the Experimental Slate Data

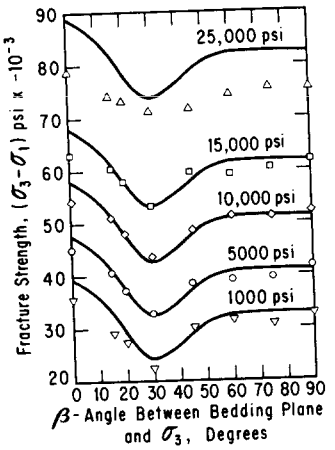

Fig. 25. Comparison of Green River Shale - 1 Data with the Variable τ_o and tan ϕ Criteria

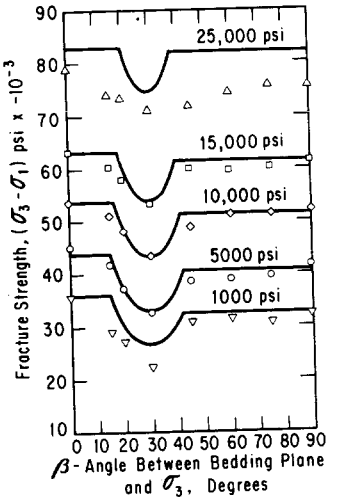

Fig. 26. Comparison of Green River Shale - 1 Data with the Walsh - Brace Theory

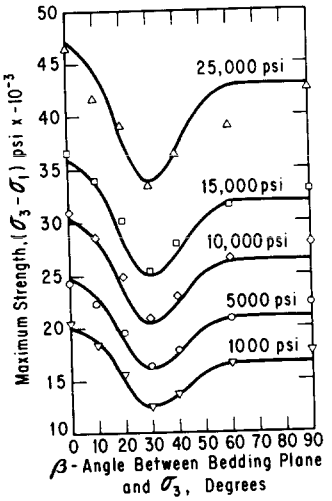

Fig. 27. Comparison of Green River Shale - 2 Data with the Variable τ_o and tan ϕ Criteria

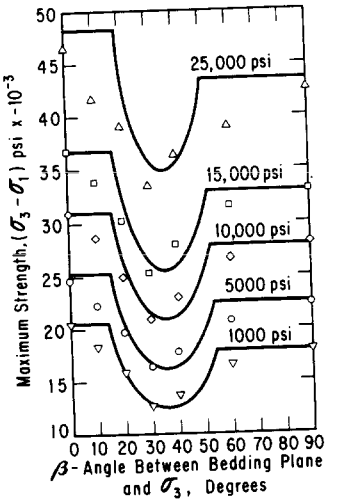

Fig. 28. Comparison of Green River Shale - 2 Data with the Walsh - Brace Theory

Fig. 29. Types of Failures Noted *

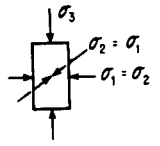

1. SHEAR
   a. Along bedding plane
   b. Across bedding plane

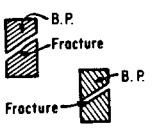

2. "PLASTIC" FLOW or SLIP
   a. Along bedding plane

3. "KINK" FLOW
   Consists of a rotation of bedding plane

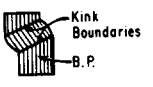

* 1. All three types noted in Slate and Green River Shale - 2 tests
2. Failures 1. & 2. noted in Green River Shale - 1 tests

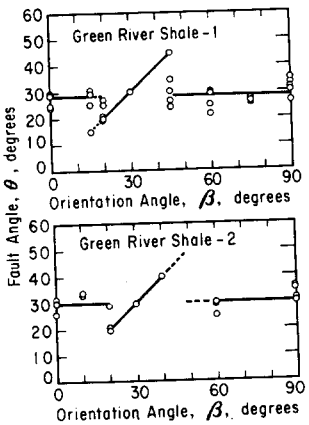

Fig. 30. Effect of the Plane of Anisotropy on the Fault Angle for Green River Shale

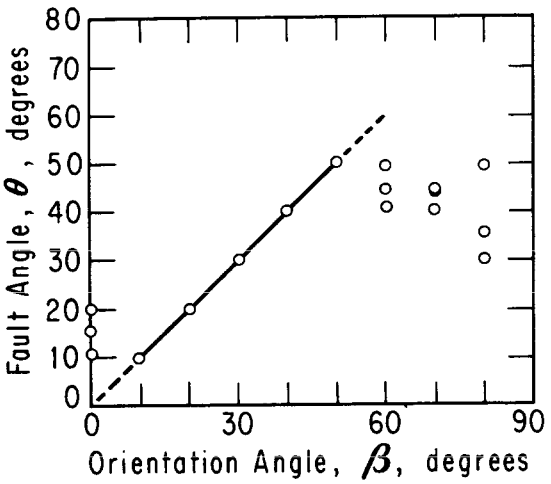

Fig. 31. Effect of Cleavage Plane on Fault Angle for Slate

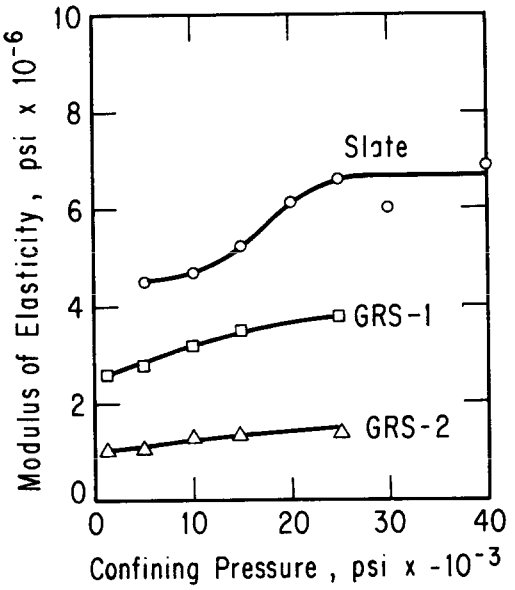

Fig. 32 Variation of the Average Modulus of Elasticity with Confining Pressure

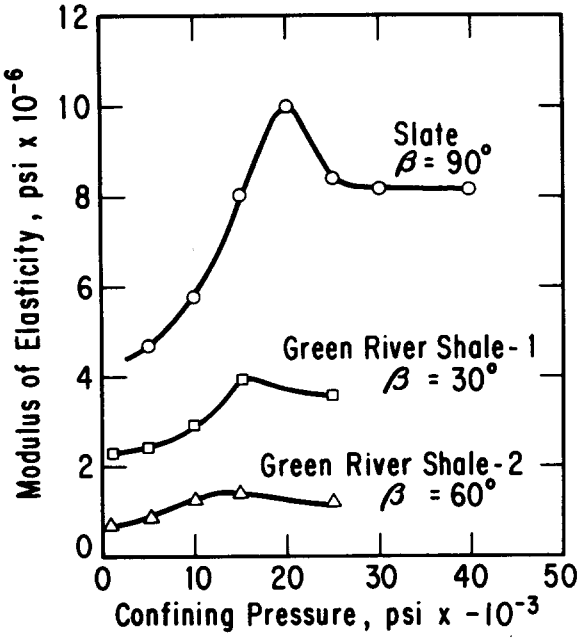

Fig. 33. Variation of the Modulus of Elasticity with respect to Confining Pressures

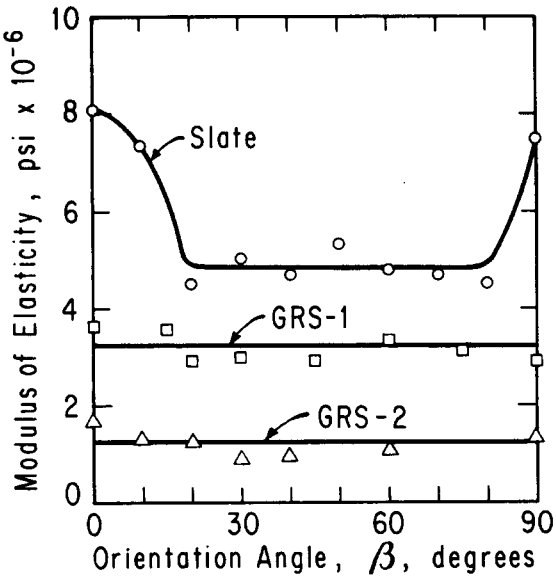

Fig. 34. Variation of the Average Modulus of Elasticity with Respect to Orientation

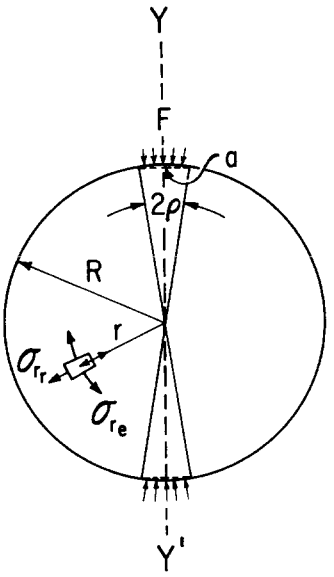

Fig. 35. **Brazilian Test Sample Under Strip Loading**

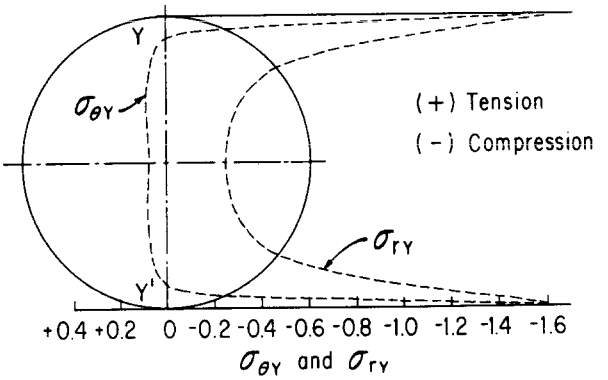

Fig. 36. Theoretical Stress Distribution Along the Line of Loading Y-Y' in a Brazilian Test Sample for Strip Load Angle $\rho = \tan^{-1}(\frac{1}{12})$, $\frac{2P}{\pi t} = 1$ (After Hondros)

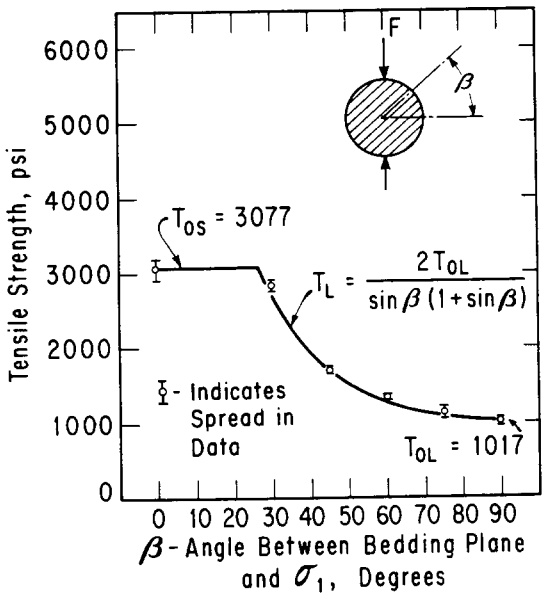

Fig. 37. Comparison of Tensile Strength Data for Green River Shale-1 with Griffith Theory

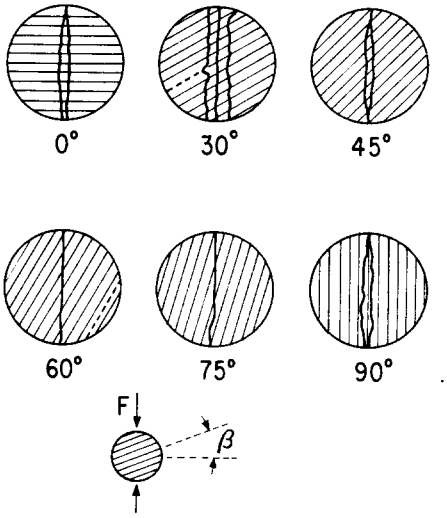

Fig. 38. Failure Modes for Green River Shale-1, Brazilian Tests at Atmospheric Pressure and Variable β